DTIC FILE COPY ②

NAVAL POSTGRADUATE SCHOOL
Monterey, California

THESIS

THE DESIGN AND INITIAL CONSTRUCTION OF A
COMPOSITE RPV FOR FLIGHT RESEARCH APPLICATIONS

by

H. Keith Parker

September 1988

Thesis Advisor: Richard M. Howard

89   1 04 011

REPORT DOCUMENTATION PAGE

1a Report Security Classification Unclassified		1b Restrictive Markings		
2a Security Classification Authority		3 Distribution Availability of Report		
2b Declassification/Downgrading Schedule		Approved for public release; distribution is unlimited.		
4 Performing Organization Report Number(s)		5 Monitoring Organization Report Number(s)		
6a Name of Performing Organization Naval Postgraduate School	6b Office Symbol *(If Applicable)* 31	7a Name of Monitoring Organization Naval Postgraduate School		
6c Address *(city, state, and ZIP code)* Monterey, CA 93943-5000		7b Address *(city, state, and ZIP code)* Monterey, CA 93943-5000		
8a Name of Funding/Sponsoring Organization	8b Office Symbol *(If Applicable)*	9 Procurement Instrument Identification Number		
8c Address *(city, state, and ZIP code)*		10 Source of Funding Numbers		

Program Element Number	Project No	Task No	Work Unit Accession No

11 Title *(Include Security Classification)* The Design and Initial Construction of a Composite RPV for Flight Research Applications.

12 Personal Author(s) H. Keith Parker

13a Type of Report Master's Thesis	13b Time Covered From To	14 Date of Report *(year, month,day)* September 1988	15 Page Count 100

16 Supplementary Notation The views expressed in this thesis are those of the author and do not reflect the official policy or position of the Department of Defense or the U.S. Government.

17 Cosati Codes			18 Subject Terms *(continue on reverse if necessary and identify by block number)*
Field	Group	Subgroup	RPV, Wortmann FX63-137 Airfoil, Composite Construction

19 Abstract *(continue on reverse if necessary and identify by block number*

A remotely piloted vehicle, similar to the U. S. Navy's Pioneer RPV, was designed and initial construction implemented for the purpose of establishing an RPV flight research program at the Naval Postgraduate School. The RPV will be used to investigate the Wortmann FX63-137 airfoil for low Reynolds applications, testing airborne avionic devices, investigate new aerodynamic phenomena of interest to NAVAIR, and serve as a transition trainer for future RPVs. Constructed primarily of composite materials, the vehicle will provide the opportunity to conduct real time/in-flight composite structural analysis. Additionally, the opportunity of using an RPV in their research, will provide the students of the Naval Postgraduate School with a unique capability limited to very few universities throughout the country.

20 Distribution/Availability of Abstract [X] unclassified/unlimited [ ] same as report [ ] DTIC users	21 Abstract Security Classification Unclassified		
22a Name of Responsible Individual Richard M. Howard	22b Telephone *(Include Area code)* (408) 646-2870	22c Office Symbol 67Ho	

DD FORM 1473, 84 MAR   83 APR edition may be used until exhausted   security classification of this page

All other editions are obsolete   Unclassified

Approved for public release; distribution is unlimited

The Design and Initial Construction of a Composite RPV for Flight Research
Applications

H. Keith Parker,
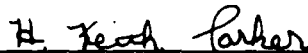Lieutenant, United States Navy
B.S., Texas A&M University, 1980

Submitted in partial fulfillment of the
requirements for the degrees of

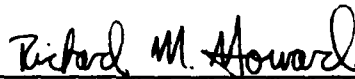MASTER OF SCIENCE AERONAUTICAL ENGINEERING

from the

NAVAL POSTGRADUATE SCHOOL
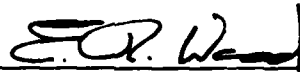September 1988

Author: _____
H. Keith Parker

Approved by: _____
Richard M. Howard, Thesis Advisor

_____
E. R. Wood, Chairman,
Department of Aeronautics and Astronautics

_____
Gordon E. Schacher,
Dean of Science and Engineering

ii

ABSTRACT

A remotely piloted vehicle, similar to the U. S. Navy's Pioneer RPV, was designed and initial construction implemented for the purpose of establishing an RPV flight research program at the Naval Postgraduate School. The RPV will be used to investigate the Wortmann FX63-137 airfoil for low Reynolds applications, test airborne avionic devices, investigate new aerodynamic phenomena of interest to NAVAIR, and serve as a transition trainer for future RPVs. Constructed primarily of composite materials, the vehicle will provide the opportunity to conduct real time/in-flight composite structural analysis. Additionally, the opportunity of using an RPV in their research, will provide the students of the Naval Postgraduate School with a unique capability limited to very few universities throughout the country.

iii

TABLE OF CONTENTS

TABLE OF SYMBOLS AND/OR ABBREVIATIONS

a_e Effective lift-curve slope, $(a_w$ or $a_t) / E$

a_t Lift-curve slope of horizonal tail

a_w Lift-curve slope of wing

$a_{[2-d]}$ Two-dimensional lift-curve slope

$a_{[3-d]}$ Three-dimensional lift-curve slope

AR   Aspect ratio, b^2/S

A_π Area upon which individual component drag coefficient is based

b   Wing span, feet

c   SMC: standard mean chord

C_D Total three-dimensional drag coefficient

C_{Dp} Parasite drag coefficient

$C_{D\pi}$ Drag coefficient based on a relevant area A_π other than wing area

C_L Three-dimensional lift coefficient

C_{Ltrim} Three-dimensional lift coefficient at trimmed condition

$\dfrac{dC_L}{d\alpha}$ Slope of C_L versus α curve

C_{Mac} Three-dimensional pitching moment coefficient about the aerodynamic center

C_{mac} Two-dimensiinal pitching moment coefficient about the aerodynamic center

C_{Mcg} Total pitching moment coefficient about the center of gravity

$\dfrac{\partial (C_M)_{cg}}{\partial \alpha_{abs.}}$ Slope of the moment coefficient curve

$C_{M\ fuselage}$ Moment coefficient due to fuselage

$C_{n\beta}$ Yawing moment coefficient with a change in angle of sideslip, β

$(C_{n\beta})_{desirable}$ Desirable value for the yawing moment coefficient with a change in angle of sideslip, β

$(C_{n\beta})_{fuselage}$ Fuselage contribution to yawing moment coefficient with a change in angle of sideslip, β

$(C_{n\beta})_v$ Primary vertical tail contribution to yawing moment coefficient with a change in angle of sideslip, β

$(C_{n\beta})_{v.t.}$ Total vertical tail contribution to yawing moment coefficient with a change in angle of sideslip, β

$(C_{n\beta})_{wing}$ Wing contribution to yawing moment coefficient with a change in angle of sideslip, β

$(C_{n\beta})_{w.p.}$ Windmilling propeller contribution to yawing moment coefficient with a change in angle of sideslip, β

$\Delta_2\, C_{n\beta}$ Secondary vertical tail contribution to yawing moment coefficient with a change in angle of sideslip, β

$\dfrac{dC_{yp}}{d\beta}$ Change in sideforce coefficient with a change in sideslip angle

D Propeller diameter, feet

E Jones edge-velocity factor, equals ratio of the semiperimeter of the surface under consideration to the span of the surface

f Modification factor from page 16 of Reference 18

f_b Basic parasite drag area, ft

$f_{cooling}$ Cooling drag modification factor

$f_{interference}$ Interference drag modification factor

$f_{landing\ gear}$ Landing gear drag modification factor

$f_{protuberance}$	Protuberance drag modification factor
f_t	Total parasite drag area, ft^2
f_{trim}	Trim drag modification factor
G	Modification factor from page 20 of Reference 16
h	Fraction of the standard mean chord, SMC, which locates the center of gravity
h_{ac}	Location of aerodynamic center of wing-plus fuselage on SMC
h_n	Stick-fixed neutral point on SMC
h_1	Height of fuselage at 1/4th fuselage length
h_2	Height of fuselage at 3/4th fuselage length
i_t	Horizontal stabilizer incidence
K_β	Modification factor from page 320 of Reference 19
K'	Induced drag factor of real wing with rest of aircraft attached
k_f	Modification factor from page 229 of Reference 19
L	Characteristic length
l	distance between wing and horizontal tail quarter chords
L/D	Lift to drag ratio
L_f	Length of fuselage, feet
l_p	Distance from c.g. to the propeller disk, feet
N	Number of propellers
R_e	Reynolds number
S_s	Projected fuselage side area, ft^2
S_w	Wing area, ft^2
V	Freestream velocity in ft/sec

V_H	Horizontal stabilizer (tail) volume coefficient
V_{trim}	Freestream velocity in ft/sec at the trimmed condition
W	Aircraft weight, pounds
W_f	Width of fuselage, feet
w_1	Width of fuselage at 1/4th fuselage length
w_2	Width of fuselage at 3/4th fuselage length
α_{abs}	Absolute angle of attack
ε	Aerodynamic twist in degrees from root to tip, measured between the zero lift line directions of the center and tip sections, positive for wash in
ε_o	Angle of downwash at tailplane during zero lift condition due to wing or foreplane
$\varepsilon^o{}_{tail}$	Angle of downwash at tailplane due to wing or foreplane
$\dfrac{\partial \varepsilon}{\partial \alpha}$	Change in angle of downwash at tailplane due to a change in angle of attack
Λ	Angle of sweepback, measured between the lateral axis and a line through the aerodynamic centers of the wing sections
λ	Taper ratio, tip chord/root chord
μ	Dynamic viscosity
π	(Circumference/diameter) of a circle $\cong 3.141593...$
ρ	Ambient density of air

ACKNOWLEDGMENT

Upon the completion of a great task, it is customary to thank those who offered encouragement and help along the way. I would like to personally thank Professor Rick Howard of the Naval Postgraduate School. His expertise and dedication to profession were a major contribution to the completion of this thesis.

A special thank you goes to my wife, ██████████ whose patience and understanding has been most supportive during my tour at the Naval Postgraduate School.

I. INTRODUCTION

Jake has been in the airwing only two months and each day continues to test the utmost of his ability. Today's mission will prove no different. The airwing is conducting a strike early this morning and Jake will follow up after the smoke has cleared to conduct bomb damage assessment (BDA), a mission which generally has a high probability of drawing hostile fire.

The ingress goes well with Jake using the terrain as much as possible to mask his presence. Once over the target area the cameras are switched on and the information is immediately satellite linked to the airwing commander onboard the aircraft carrier.

During the egress, twenty miles from feet wet, Jake is detected and draws hostile anti-aircraft fire. A high-explosive projectile hits the fuel tank and the subsequent explosion destroys the aircraft. The news that Jake has been shot down spreads throughout the carrier in short order, yet there seems to be no distraught faces, no remorse. How can this be? Maybe it's because he hadn't been on board long and was not well known. No, that's not it at all. There is no sadness because a pilot has not been lost. For you see, Jake was the code name for the remotely piloted vehicle (RPV) recently acquired by the U. S. Navy. Even though the RPV was lost, the mission was a success. All the necessary information had been linked to the carrier, no human life had been lost and a multi-million dollar aircraft had not been destroyed. Jake was a relatively inexpensive, expendable system designed to perform a variety of functions too difficult or too dangerous for manned aircraft.

II. BACKGROUND—HOW AND WHY RPVS CAME INTO EXISTENCE

This scenario typifies the sort of mission that can be performed by systems based on today's unmanned air vehicles. There are dozens of missions that do not require full-time human control and these could potentially be performed by unmanned aircraft. Such missions might include those which are hazardous, monotonous, or beyond human endurance. In extreme cases, some missions are almost certain to result in the destruction of the vehicle. Even when the risk and the cost of a manned mission are smaller, the use thereof may still not be justified by the results. There are other factors to consider in certain specialized operations. For example, an amorphous heap of wreckage cannot be prosecuted for espionage. [Ref. 1:p. 1771]

The United States has been involved in the use of RPVs since 1917; however, this use has been slight and generally restricted to target drones. The most extensive U. S. use of RPVs to date was during the Vietnam conflict. According to CDR Parker [Ref. 3:pp. 12-13] between 1964 and 1965, more than 3,435 RPV sorties were flown over Southeast Asia. Missions included photo reconnaissance, electronic intelligence gathering, bomb damage assessment, psychological warfare(propaganda leaflet dropping), and electronic warfare. The program produced excellent results in Vietnam, but was dead within a few years of the ceasefire, for a number of reasons. Budgets were tight and the USAF preferred to spend its money on badly needed manned aircraft. The jet powered drones, with their launch/director and retrieval aircraft, were not cheap to operate and the use of

2

unmanned aircraft in other theaters, such as a densely populated, peacetime Europe, created numerous problems. [Ref. 1:p. 1772]

A. APPLICATION—MILITARY AND CIVIL USES

Dismissed for several years as expensive toys of little tactical value, remotely piloted vehicles are finally earning a major role in military thinking [Ref. 2:p. 38]. RPVs have recently drawn major interest from military planners because of their expanded capabilities: a degree of miniaturization that allows highly advanced sensors to be integrated into small size and low weight packages at a low cost. For areas in which it can be applied, this is an attractive alternative to the increasing costs of major weapon systems.

The increasing potency of threat weapons has generated a need to reevaluate the use of our scarce, high-cost military resources in a high-threat environment. Because of its relatively low cost, high survivability based on small size, inherent flexibility, and capability developed through state-of-the-art technology, the remotely piloted vehicle has become most attractive for expanded military application.

Dr. Edward Teller, father of the nuclear age, said, "The unmanned vehicle of today is a technology akin to the importance of radar and computer in 1935" [Ref. 3:p. 12].

One country that has aggressively pursued the development of RPVs for military use is Israel. That Israeli investment paid off in June 1982, during the invasion of Lebanon. The relatively simple Mastiff and Scout mini-RPVs built by Mazlat (Tel Aviv) led the advance into the dangerous Bekaa Valley, undertaking key decoy work and gathering reconnaissance data on Syrian-manned, Soviet-made surface-to-air missile sites. Flying into the valley, the RPVs emitted electronic

signals that mimicked radar signals from Israeli jets. When the Syrians activated their short-range radars in response to the perceived threat, the RPVs identified and passed on the missile site locations and characteristic radar emissions, enabling Israeli smart missiles to destroy 29 SAM sites in a single hour. With the enemy air defense blinded, Israeli fighters then swept into the valley for cleanup operations, as the RPVs monitored bomb damage and the movement of Syrian forces. [Ref. 2:p. 40]

RPVs do not represent a panacea for military problems, but they do provide an extra dimension of force that, in conjunction with more traditional military technology, can increase the effectiveness of tactical operations [Ref. 2:p. 43].

Two decades ago, on the limited occasions when the U.S. military used unmanned aircraft, it relied mainly on medium-size, or midi RPVs. Today the services show growing interest at the two extremes. Mini-RPVs, weighing under 600 pounds and derived largely from advancing model and homebuilt aircraft technology, have attracted wide attention. Military planners are also experimenting with maxi-RPVs, which tip the scales at between 5000 and 15,000 pounds and are designed to fly at altitudes of 50,000 to 80,000 feet for periods of days.

The air vehicle itself represents just one component of an RPV system. Launch and landing equipment determines the nature of payloads that a specific craft can carry; different RPVs can take off from airfields, hastily prepared strips, trucks, and ships and end their missions by landing on dirt roads, dropping by parachute, or flying into nets. Just as critical to an air vehicle's mission is its ground control station. A typical RPV system consists of a ground control station, perhaps two

portable control stations and two remote receiving stations, a single launcher and associated equipment, and anywhere from three to a dozen air vehicles.

The key to RPVs' success, however, is what resides in the air vehicles, in the form of sensors and other electronic devices. Cameras, forward-looking infrared radar (FLIR) for night vision, and communications equipment for vehicle-to-ground data links can be packaged inside airframes so small that they almost inevitably evade radar detection.

Given the sophistication of such hardware and associated software, RPVs can carry out a broad spectrum of tasks. The most fundamental is the oldest of all military missions: peering over the next hill to see what the enemy is doing and how he is doing it. But they can also carry out a passel of new missions strictly geared to modern warfare. In the reconnaissance role, they can survey battlefields for mines before attacks and assess damage after--by night as well as by day. As spotters, they can bracket targets precisely for artillery and naval guns, and guide smart missiles to military targets by illuminating the targets with lasers. They can perform a variety of communications chores, from acting as radio relay towers to jamming enemy communications and radars and eavesdropping on enemy signals intelligence. And the vehicles can take on such active task as dispensing flares, dropping small bombs, and acting as decoys to protect friendly aircraft. [Ref. 2:p. 38]

The technology of modern military aircraft appears to be advancing far faster than the ability of human pilots to oversee it. As an example, the USAF currently requires all their F -16 pilots to be centrifuge rated at nine g's to help identify those pilots who are prone to g induced loss of conscious (GLOC). "We're finding more and more that the weakest link in an aircraft is the pilot," says Allen Atkins, head of

DARPA's aerospace technology. Across the Atlantic, NATO's Advisory Group for Aerospace Research and Development (AGARD) is examining the technology and cost-effectiveness of an unmanned aircraft capable of maneuvers involving forces too high for human pilots to withstand. A ground controller would share the role of pilot with on-board artificial intelligence; the controller would make the key decisions while the computer would actually fly the plane. [Ref. 2:p. 43]

For the majority of today's military missions unmanned air vehicles are needed to complement, not replace, manned systems. RPV complementary capability was most vividly demonstrated by the Israelis in the Bekaa Valley. Their use within a carrier battle group to perform a variety of the previously mentioned tasks, would in effect, increase the strength and capability of the airwing without requiring precious deck or storage space on the aircraft carrier. RPVs can also perform a wide variety of civil uses such as fire detection and wildfire mapping, fishing and law enforcement, security of high-value property, pipeline patrol, storm research, and various agriculture duties. Appropriately-equipped RPVs can sense radiation, as well as chemical or biological contamination. [Ref. 4:pp. 10-11]

B. CURRENT U. S. NAVY RPV APPLICATIONS

As a result of a demonstration proving the RPV's capabilities, Naval Air Systems Command was directed in July 1985 by former Secretary of the Navy John Lehman to implement a RPV program using off-the-shelf technology. Doing so would enable an RPV unit to be deployed to the fleet as soon as possible for intelligence gathering and fleet support.

In order to find the most effective and efficient technology being used, competitive tests were conducted from October through December of 1985. The conclusion drawn upon the completion of these test was that the Pioneer, an

unmanned air vehicle marketed by AAI Corporation/Mazlat LTD was the best suited for the Navy's needs. [Ref. 5:pp. 15-16]

The Pioneer air vehicle has a wing span of 16.9 feet and a maximum gross weight of 419 pounds. The vehicle is propelled to its maximum speed of 115 miles per hour by a Sachs SF2-350 (26HP) horizontally-opposed twin cylinder, two-stroke engine. Several payload packages can be employed within the 100 pound payload limit. Options currently available include the gyro stabilized MKD-200 high-resolution daylight TV camera or the MKD-400 FLIR for night or reduced visibility operations. [Ref. 5:p. 16]

Mission success in a high-threat environment is very much dependent on the survivability attributes of the vehicle conducting the mission. Survivability of the Pioneer is enhanced by its small size, low visual signature, jam resistant data link, and low radar/IR signature. In addition, the Pioneer's endurance time and altitude capability make it a viable option for many Naval applications.

Installation of the RPV system aboard the USS Iowa (BB-61) began in April 1986. A rocket-assisted takeoff capability was introduced as the battleship's answer to catapult launches and a net was designed for shipboard recovery. However, the Pioneer's introduction has not been without casualty. During the system's first deployment aboard the Iowa in 1986, four out of five air vehicles were lost. After the first cruise, the Navy and AAI formed so-called "tiger teams" of specialists to work on the problems which had been identified, and air operations resumed shortly thereafter. The Pioneer was deployed aboard the Iowa again in July 1987 and has been flying ashore and afloat ever since. To date the system has acquired over 600 flight hours of which more than 60 hours have been at night. The first U. S. Marine Corps companies have been formed and have conducted night fire

support exercises with the optional thermal imager. During the latest trials onboard the battleship Iowa, the RPV logged more than 110 flight hours, 20 of which were flown at night employing the forward-looking infrared sensor. [Ref. 5:p. 16 & Ref. 6:p. 1025]

A Navy baseline review of the AAI/Mazlat Pioneer remotely piloted vehicle program has endorsed the concept of a short-range unmanned vehicle for over-the-horizon surveillance and targeting and recommended procuring the system in quantity.

Pending Department of Defense approval, the Navy will pick up its option to procure four more Pioneer systems to support an operational evaluation in 1989. Each system consists of eight RPVs, one ground control station and a tracking control unit. A full-scale production decision is scheduled in Fiscal 1989. Eventually, the Navy wants to procure 43 systems, including 344 RPVs, for over-the-horizon targeting, surveillance, and support of amphibious operations.

The base line review follows extensive field testing of the system by the Navy and the Marine Corps that was intended to determine whether there was an operational need for a short-range RPV system and what the final configuration should be. [Ref. 7:p. 25]

The Pioneer RPV system has performed remarkably well and has proven quite cost effective considering it was an off-the-shelf system that was intended to be a stop-gap solution to an existing problem and that it was employed without the usual operational test and evaluation required of major Navy systems. There have been several problem areas identified, however, and work is presently being done to correct these deficiencies and to implement improvements. Some of the critical issues include finding an alternative-fuel engine capable of running on JP-5 or

diesel fuel to replace the current engine. A command/control data link needs to be developed that will expand the effective control range beyond the 100 nautical mile limit. It is considered by some that the Pioneer air vehicle is slightly deficient in pitch authority, requiring a rather lengthy and flat glide slope be used during recovery, thereby increasing the time spent in a critical transition region. Such a deficiency also necessitates that a higher approach speed be utilized which in turn increases the danger of the recovery to personnel and to the air vehicle.

The Navy has identified several low Reynolds number airfoils, such as the Wortmann FX 63-137 airfoil, which might offer superior performance over those currently in use, especially at conditions of high lift encountered in the landing mode.[1] With the use of such an airfoil and some "fine tuning " of the stability parameters, the handling qualities of the Pioneer RPV or a similarly configured vehicle could possibly be improved upon.

---

[1]LCDR R. Fisher, Pacific Missile Test Center, conversation at NPS, 26 Nov. 1987.

9

III. THE RPV PROGRAM AT THE NAVAL POSTGRADUATE SCHOOL

The Department of Aeronautics and Astronautics at the Naval Postgraduate School is expecting delivery of an RPV similar to those currently operational in the U. S. Navy. Anticipating this delivery, it is necessary to develop a smaller training aircraft. This craft will serve as a transition trainer and until the full-scale vehicle is delivered and made operational, it will also serve as the primary flight research test bed.

The primary research objective of this study is the design and initial construction of an RPV flight test vehicle. The vehicle will be used to investigate the feasibility of using the Wortmann FX 63-137 airfoil, as well as improving the stability and control characteristics of the Pioneer RPV. Being built primarily of composite materials, it will also serve as a structural research vehicle, whereby more insight can be gained in real time/in-flight composite structural analysis. The craft will also be used to test and evaluate airborne avionic devices such as autopilots, rate gyros and accelerometers. The RPV will be used as a platform for testing other research projects in the real flight environment at a scale not limited to those of a wind tunnel. High lift devices, winglets, boundary-layer control methods, variable geometry surfaces, multiple lifting surface configurations, innovative control surfaces, and improved propellers represent areas of interest that may be applied to the RPV or to other aircraft. The use of the RPV allows researchers the ability to investigate new aerodynamic phenomena in a relatively hazard-free testing environment at a fraction of the cost required for full-scale research and development.

This project is not intended to break new ground in design theory or in RPV technology, but to use proven design techniques, along with existing technology and as many off-the-shelf products as feasible, to facilitate obtaining an operational test vehicle in a reasonable amount of time. The design and construction of a project of such magnitude is expected to extend beyond the time allotted for one student's thesis research. Therefore it will be an on-going project requiring subsequent work of several students to achieve completion.

A. THESIS PROJECT BENEFIT

In addition to performing as a transition training aircraft, an inflight structures laboratory and a platform for testing Naval Postgraduate School research projects in a real flight environment, the RPV can be used to investigate aerodynamic phenomena of interest to NAVAIR with application to the RPV or other aircraft.

One must remember that the goal of the Naval Postgraduate School is to serve the Navy by educating its officers and preparing them for their technical roles in the Navy of today and the future Navy of tomorrow. It is felt that the opportunity of using a RPV in their research at NPS will not only offer the students a resource limited to very few universities, but will give them the opportunity for direct experience in flight research and flight test techniques. Experimental research programs are necessary to confront the student with the task of program management and to provide he or she with an avenue for expanding their technical expertise in a way beneficial to themselves and the U. S. Navy.

B. SIMILAR CONCURRENT/PREVIOUS RESEARCH

Two thesis projects currently being researched at the Naval Postgraduate School involve investigation into the performance of low Reynolds number airfoils with high freestream turbulence. This work involves wind tunnel testing of various airfoil models (including the Wortmann FX 63-137) with generated turbulence. One project involves force and wake measurements, and another involves hot-wire measurements in the airfoil boundary layer to construct velocity profiles for comparison to computer predictions.

In addition, wind tunnel component testing studies are planned for the NPS wind tunnels. Areas to be studied include:
- New RPV airfoils for improved endurance/dash speed performance
- Control and high-lift devices for improved maneuverability and lower approach speed
- Boundary-layer control devices (vortex generators) for good low Reynolds number performance in a degraded flight environment

Stollery and Dyer from the College of Aeronautics in Cranfield, England, have conducted wind tunnel test on seven different airfoil sections at the appropriate low speed conditions in which RPVs fly. The Wortmann FX 63-137 was among the seven airfoils tested and it was found that the Wortmann section gave a substantially high value of maximum lift coefficient and maintained good lift to drag ratios over the whole incidence range. [Ref. 8:p. 11]

The results of Stollery and Dyer prompted the Royal Aircraft Establishment (RAE) at Farnborough to build an instrumented full-scale wind tunnel model of the RPV used in the initial test with the capability of being tested using alternative wings. One wing had the original flat bottom section originally used on the RPV and the other had the Wortmann section. The results confirmed that the Wortmann section gave an increased value of C_{Lmax}. The drag of the complete aircraft was

12

similar using either wing at low angles of attack; however, as the angle of attack was increased (C_L greater than 1.2), a substantial increase in performance was realized by using the Wortmann FX 63-137 airfoil section. [Ref. 8:p. 11]

It is well known that, under the low Reynolds number conditions typical of RPV flight, airfoil performance is not only a function of Reynolds number but within a limited range is also susceptible to airfoil shape, including roughness, freestream turbulence and background noise levels [Ref. 9:pp. 253-256]. One noteworthy example involves the small single-engine Quickie, a tandem-wing homebuilt aircraft. Because of its small size, low speed, and airfoil shape the aircraft has a substantial amount of laminar flow on its flying surfaces. As more of these aircraft came into service, pilots began to report a new phenomenon. When encountering a light rain, the aircraft changed pitch trim, tending to nose down, and required more back stick pressure to maintain level flight. The problem has been attributed to the moisture (roughness) on the airfoil causing a reduction in the amount of laminar flow achieved thereby leading to premature flow separation and subsequent loss of lift for the particular airfoil used on the front wing. [Ref. 10:pp. 305-309] Roughness can be caused by many things but most notably, either from damage or by interference from slots, gaps, cavities, or bumps. In conjunction with the RAE study mentioned previously, Davidson [Ref. 8:p. 11] studied the effects of roughness on the performance of three wing sections used in the study by Stollery and Dyer. A roughness strip was fitted to Wortmann FX 63-137, Gottingen 797, and NACA 64-418 sections and the sections were tested at a chord Reynolds number of 1×10^6. For each section tested the lift was degraded and the drag increased; however, the Wortmann section still retained its superiority by having the best C_{Lmax} and the highest L/D ratio.

The final phase of this study involved instrumenting and measuring the flight performance of the RPV, first using the original wing and then with a new wing utilizing the Wortmann section. The flight data lift curves clearly showed the improvement due to the wing utilizing the FX 63-137 section. [Ref. 8:p. 12]

Some possible benefits of the Wortmann FX 63-137 airfoil, as evidenced by this study, include a high value of C_{Lmax} which can reduce take-off and landing speeds or allow a greater payload to be carried. If the landing speed can be significantly reduced, then an alternative ship board recovery method may prove feasible. Upon comparison of the two-dimensional data with the three-dimensional flight data, it is apparent that the "degradation" caused by the fuselage effects and the roughness is small. In particular, the magnitude of the benefit in going from the "old" to the "new" wing section was maintained throughout.

IV. DESIGN METHOD

The design of this RPV was unique in that there was no specific mission which dictated the design. Unlike most RPVs, this one was not designed to fly a specified range or loiter for a predetermined number of hours. The primary mission of this RPV is to serve as a transition trainer for the Mastiff/Pioneer RPV the Postgraduate School is expecting to receive and to perform as a test vehicle for improvements to the Pioneer; therefore it is these factors which drove the design. To successfully perform its mission, the air vehicle must be statically and dynamically stable in addition to having very forgiving flight characteristics. It is also pertinent for the correlation of design improvements, that the configuration of the vehicle be quite similar to that of the Pioneer. This requires that the aircraft have a central fuselage pod connected to the empennage by a twin-boom arrangement and that a pusher configuration be adopted. An additional goal was to keep the design simple to facilitate the construction process and to achieve a light vehicle.

The first step in the design process was to obtain data on the Pioneer. Some general specifications such as length, span, wing area, and gross weight were obtained as were some photographs. The photos were scaled to provide estimates for design parameters such as tail volume ratio. The general design specifications were initially scaled to produce a vehicle roughly two-thirds the size of the Pioneer. These dimensions were then slightly altered in an attempt to size the vehicle for its intended payload and to insure a stable platform.

RPVs have only been in use to a large extent for a few years; therefore there does not exist a large quantity of historical data or design trends upon which to base a design. To facilitate the design process a reasonably accurate method was used.

15

This method consists of gathering data and photos of current RPV designs similar in configuration to the Pioneer. As with the Pioneer data, this information was scaled to determine design estimates, that when looked at together might show some design trends. The result of this analysis is contained in Table 1. To determine if these results were feasible for an aircraft design, they were compared to "design trends" and guidelines common in single engine homebuilt and general aviation aircraft (Table 2). These "design trends" and guidelines were obtained from Roskam [Ref. 11:pp 143, 191, and 192] and Stinton [Ref. 12:pp. 414 -428] in addition to general design information obtained from Raymer's aircraft design notebook [Ref. 13:Chapter IPG], which has been used as a textbook in the aircraft design course taught at the Naval Postgraduate School.

When the correlation of this data was completed the second iteration of the general design parameters was obtained. A listing of the parameters is contained in Table 3.

TABLE 1. VARIOUS RPV STATISTICS

RPV	fuselage length / total length	c.g. location / total length	moment arm / total length	S h.t. / S w
Pioneer	0.613	0.363	0.536	0.100
Cyclone	0.613	0.350	0.506	0.100
Teledyne Ryan 410	0.651	0.417	0.493	0.143
Stabileye	0.572	0.368	0.501	0.264
LAURA-twin boom	0.773	0.538	0.407	0.092
Northrop-twin boom	0.455	0.269	0.626	0.169
Compass Cope	N/A	0.462	0.452	0.084
AVERAGE	**0.613**	**0.395**	**0.503**	**0.136**
NPS RPV	0.668	0.428	0.508-horz.tail / 0.520-vert. tail	0.192

17

TABLE 1. - (cont.)

RPV	$\dfrac{S\ v.t.}{S\ w}$	Aspect ratio	Volume h.t.	Volume v.t.
Pioneer	0.131	9.1	0.319	0.036
Cyclone	0.131	9.1	0.331	0.051
Teledyne Ryan 410	0.206	11.45	0.444	0.073
Stabileye	0.175	5.79	0.634	0.071
LAURA-twin boom	0.087	21.05	0.343	0.015
Northrop-twin boom	0.174	6.94	0.909	0.117
Compass Cope	0.052	20.19	0.330	0.009
AVERAGE	**0.136**	**11.95**	**0.473**	**0.053**
NPS RPV	0.102	9.2	0.652	0.039

TABLE 2. REFERENCE SOURCE GUIDELINES

Reference	Volume h.t.	Volume v.t.	$\dfrac{\text{moment arm}}{\text{total length}}$	$\dfrac{S_{v.t.}}{S_w}$	$\dfrac{S_{h.t.}}{S_w}$
Roskham	0.467-0.667	0.036-0.044	-	0.080-0.102	0.182-0.213
Stinton	0.300-0.650	0.015-0.060	-	0.075-0.085	0.160-0.200
Raymer	0.500-0.700	0.04	0.45 x fuse. length	-	-

19

TABLE 3. NPS RPV SPECIFICATIONS

Total Length	8.304 ft.
Fuselage Length	5.550 ft.
Wingspan	11.500 ft.
Wing Area	14.375 ft.^{2}
Wing Chord	1.250 ft.
Wing Aspect Ratio	9.200
Gross Weight (est.)	120 lbs.
Payload Capacity (est.)	50 lbs.
Wing Loading (est.)	8.347 lbs./ft.^{2}
Cruise Speed (est.)	75 mph
Stall Speed (est.)	48 mph
C.G. Location (est.)	3.550 ft.
Horizontal Tail Span	3.890 ft.
Horizontal Tail Chord	0.708 ft.
Horizontal Tail Area	2.760 ft.^{2}
Horizontal Tail Aspect Ratio	5.500
Horizontal Tail Moment Arm	4.221 ft
Horizontal Tail Volume	0.648
Vertical Tail Span	1.250 ft.
Vertical Tail Chord	0.575 ft.
Vertical Tail Area	1.467 ft.^{2}
Vertical Tail Aspect Ratio	2.130
Vertical Tail Moment Arm	4.321 ft.
Vertical Tail Volume	0.038

A. INTERMEDIATE DESIGN PROCESS

At this point in the design process the aircraft was divided into six different categories and each category was analyzed separately to determine the approximate size of the individual components. The six categories included the fuselage, wing, horizontal tail, vertical tail, landing gear and the engine/propeller system.

1. Fuselage Design

The fuselage size of the various RPVs studied was quite varied and appears to depend very much on the amount and type of avionics the air vehicle is desired to carry. Several very important aspects of fuselage design considered were (1) the location of the center of gravity, (2) the volume required for the desired avionics package and fuel load, (3) how fuselage size and shape affects parasite drag, airflow through the propeller, and engine cooling air, (4) the loads imposed by the wing spar and engine mount upon the fuselage structure, and (5) the affect the fuselage design has upon aircraft stability.

From the initial design process it was determined that the overall fuselage length would be 99.45 inches with the fuselage pod itself being 66.65 inches in length. The center of gravity of the fuselage was chosen to lie at 42.65 inches from the nose. This design location is 42.8 percent of the total fuselage length. The average location of the c.g. of the nine RPVs analyzed was 43.48 percent. This was an arbitrary location decided upon by a rough estimation of component location and weight. As project work progresses, actual components purchased, and structure completed, a detailed weight and balance summary will be required to determine the actual c.g. location. The payload, fuel, or ballast can all be used to move the actual c.g. to the desired design location if necessary.

It was determined that the instrumentation to be incorporated in this vehicle would roughly fit within an area six inches wide by twelve inches long by six inches tall. It was also estimated that three gallons of fuel would be sufficient to conduct all missions required of this RPV. For a fuselage fuel tank approximately 251 in.^{3}/ gallon are required to contain the fuel [Ref. 13:p. AVP-3]. This equates to approximately 753 in.^{3} for the fuel tank volume. To prevent the c.g. from shifting as fuel is burned it was decided that two interconnected fuel tanks, located an equal distance from the design c.g. would be used. These tanks could be fabricated from welded aluminum or stainless steel; however, the lightest tank design would incorporate the use of composite materials. Figure 1 shows typical construction of such a fuel tank. An initial estimation for the size of the fuel tanks is 10 inches wide by 6.5 inches long by 6 inches tall.
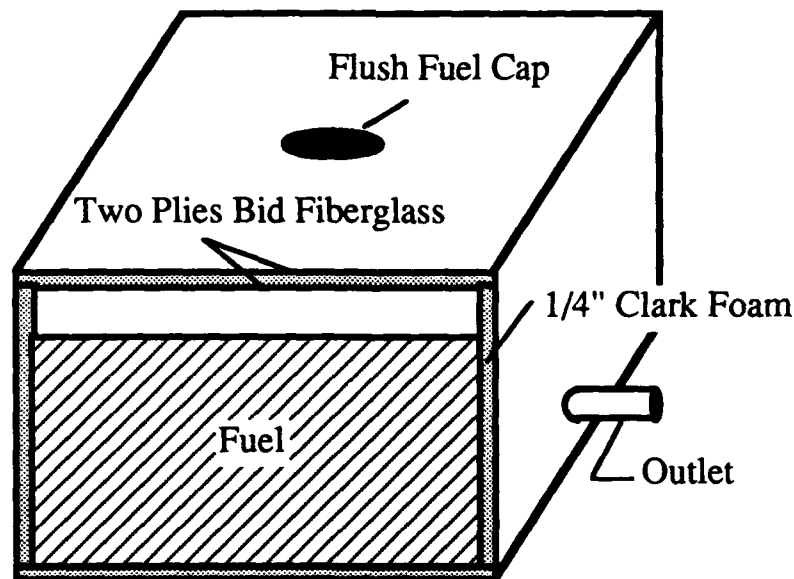

Figure 1. Fuel Tank Cross Section

Since the volume required for the avionics and the fuel tanks was relatively small, it became apparent that the diameter of the fuselage would become a function of the engine diameter, not of the avionics package or fuel load. It was decided that the Limbach L275E engine would be used to provide the propulsion for this design due to its high power to weight ratio and in addition to the fact, that it has been used with much success by the Israeli army to power the Mastiff RPV. Quick calculations showed this engine to provide more than enough power for this design; therefore the engine will be operated at a reduced throttle setting to increase propeller efficiency and to reduce engine wear. The reduced RPM will also subject the airframe and avionics to less damaging vibration. Sufficient funds to purchase the engine were not available during this conceptual design stage; therefore full-size blueprints of the engine were obtained upon which to base the design. The drawing indicted that this engine is roughly 15 1/2 inches wide, 7 1/2 inches long and 7 3/4 inches tall. An oval shape 16 inches in width and 12 inches in height was selected as the firewall dimension because it represented enough area to provide adequate cooling with the engine properly baffled without being so large to severely restrict airflow through the propeller. Since the engine is so short, the design requires that a prop extension approximately 2 inches in length be used between the crankshaft hub and the propeller in an attempt to give sufficient length to the engine cowling so that it can be reduced from the large oval shape at the firewall to an oval shape approximately 11 1/2 inches wide and 5 3/4 inches tall at the propeller hub. This reduction should reduce drag, minimize the propeller disk area blocked by the fuselage/cowling and lessen the cyclic loading of the propeller disk. To minimize frontal area, and therefore drag, it was decided to make the nose area of the fuselage large enough to accommodate only a small video camera should

23

one be desired to be added in the future. The final configuration of the fuselage is a 12 inch by 16 inch oval at the firewall which gradually tapers to a 1/4 inch pitot tube in the nose while retaining a somewhat oval shape throughout most of the fuselage length.

The section on fuselage construction contains drawings and details on dimensioning and explains the construction method used to fabricate the fuselage. Ideally the fuselage design would be analyzed to determine the stresses being imposed upon the structure. However, the design incorporates a unique composite construction method popular with homebuilt aircraft builders, which to properly evaluate requires the use of a finite element analysis. Since such an analysis is not part of this study, observations were made of several current small homebuilt aircraft designs. From this observation, a conservative estimation was made to determine the size of the fuselage members. Should a more detailed analysis be desired, a separate thesis could be conducted whereby the fuselage would be analyzed using a finite element analysis. Additionally, when the structure is completed a static load test will be conducted to ensure adequate structural strength and to validate any finite element analysis.

The stability analysis, including that contribution made by the fuselage, is contained in the section entitled "Air vehicle stability"; additionally, the details for landing gear and empennage design are also contained within the respective sections.

The overall fuselage configuration can be observed in the three-view drawing Figure 2, in addition to the more detailed drawing of Figure 3, which shows typical cross-section fuselage construction.
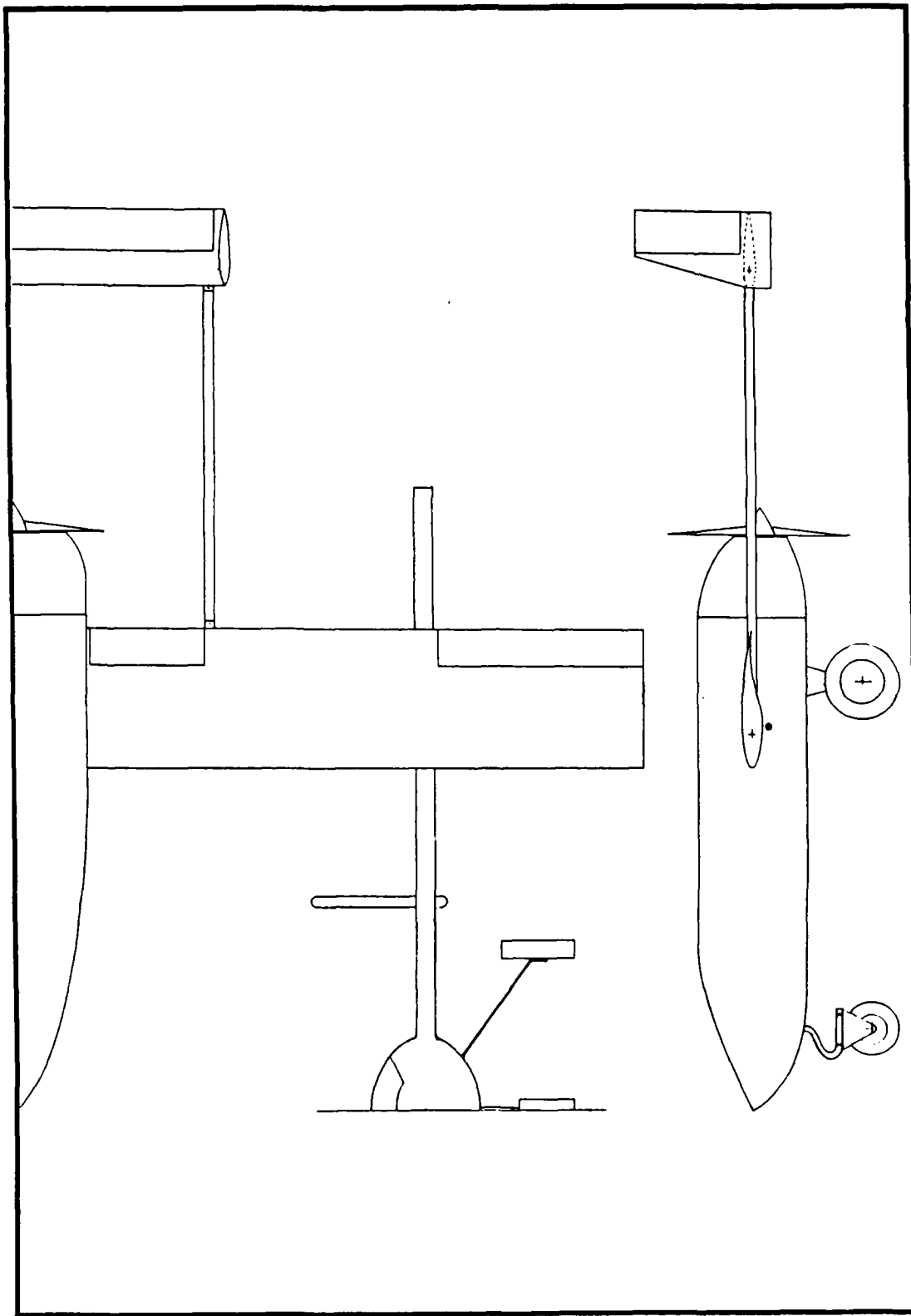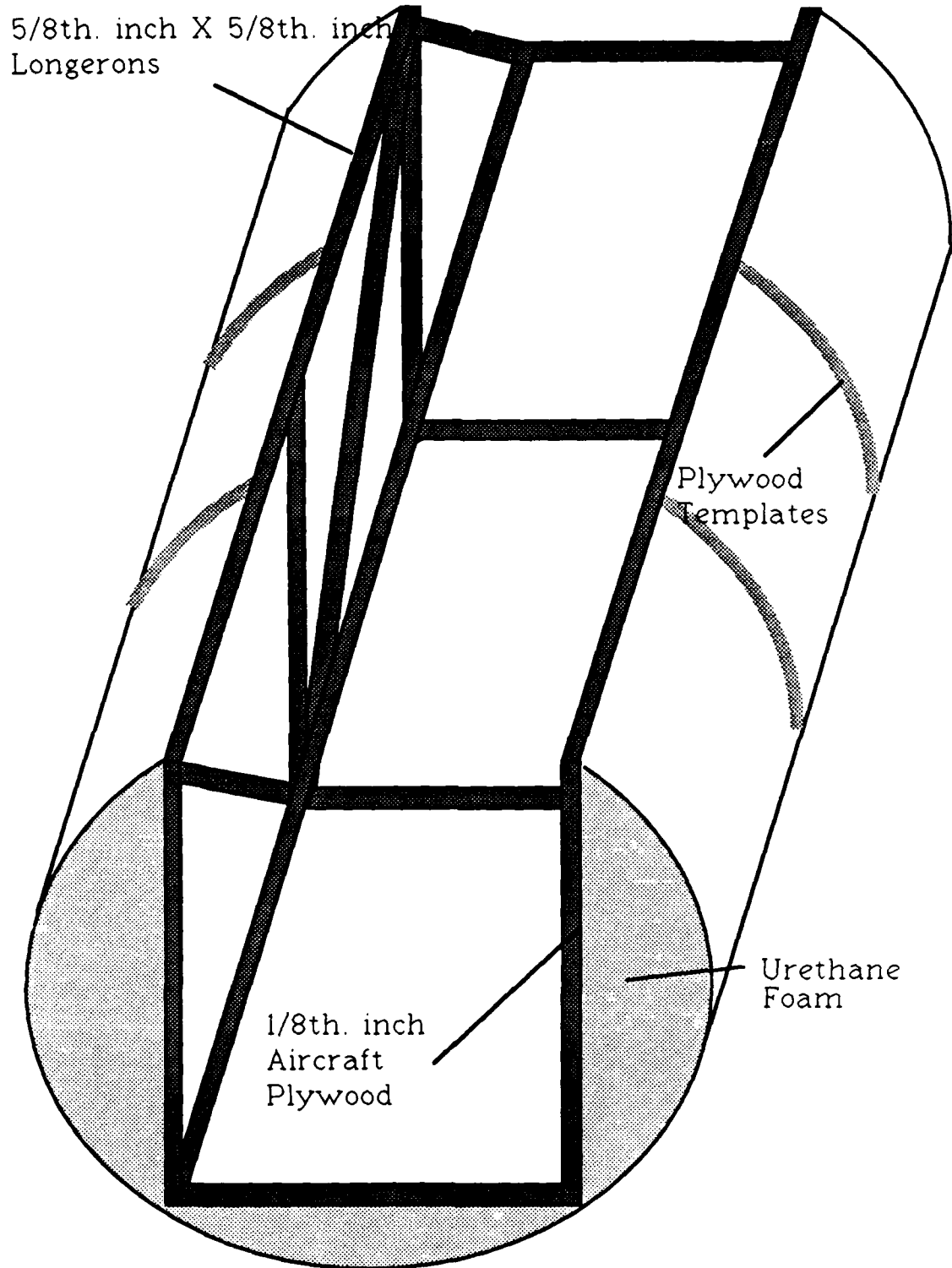
Figure 2. NPS RPV (3 View Drawing)

5/8th. inch X 5/8th. inch
Longerons

Plywood
Templates

Urethane
Foam

1/8th. inch
Aircraft
Plywood

Figure 3. Typical Fuselage Cross Section

2. Wing Design

In order to facilitate construction, to keep the design simple, and to achieve a stable trainer platform, a non-tapered rectangular wing planform was selected. A span of 11.5 feet was selected because that was roughly two-thirds that of the Pioneer RPV. During the analysis of RPV statistics the decision was made to use an aspect ratio of approximately 9.0 in order that severe adverse yaw problems could be avoided and also to minimize structural requirements. A chord length of 1.25 feet was selected, which, upon calculation, yields an aspect ratio of 9.2 and a wing area of 14.375 ft.^{2} Additionally, the wing was constructed without any washout incorporated. As previously mentioned, the Wortmann FX 63-137 airfoil was selected because of its outstanding performance at the low Reynolds number conditions typical of RPV flight.

For roll control purposes, the wing is equipped with a single pair of ailerons located on the outboard 22 inches of each wing. With a chord of 4 inches, each aileron has 90 in.^{2} of area. This provides an aileron to wing surface area ratio of 0.086 which falls within in the guidelines that an aileron should have a chord aft of the hinge line of 15 to 25 percent of the wing chord and a total area (both ailerons) of about 7 to 10 percent of the total wing area [Ref. 14:p. 59]. A pair of plain flaps are incorporated for glide path control as well as for future research in control mixing and other innovative control surface applications. Each flap has a 4 inch chord and a 12.5 inch span which equates to 50 in.^{2} of area for each flap. The flaps are located 47.85 to 60.35 inches inboard of the wing tip.

The wing aerodynamic center and the aircraft center of gravity were estimated as 0.25 chord and 0.30 chord respectively [Ref. 12:p. 418].

To reduce the required storage/maintenance area and for ease of handling/transportation to the flying site, the wing was constructed as two separate panels. The wings are inserted and bolted into a common spar box which is permanently mounted within the fuselage. This arrangement is popular with many sailplanes and homebuilt aircraft flying today. Approximately 21.5 inches either side of the aircraft centerline, an aluminum housing tube was mounted within the wing structure during construction. (Figure 4) The housing serves as the link between the wing/fuselage pod combination and the empennage. A structural aluminum tube is slid into the wing housing tube, then is either pinned or bolted in place. A similar housing exists on the horizontal tail, thereby securing the empennage to the rest of the aircraft. This arrangement is unique in that the stability characteristics of the aircraft can readily be changed by simply changing the length of the structural tube.

The wing was fabricated using "moldless" composite construction. The details explaining this method of construction are contained in the section on wing construction. Structural analysis of the wing and spar box was conducted by using two computer programs named SPAR and AIRFOIL PLOT contained in Hollmann's design textbook. [Ref. 15:pp. 139-163]

SPAR, using a constant pressure distribution over the wing, calculates the shear load, wing bending moment, and sizes the spar cap and shear web thickness of the wing. AIRFOIL PLOT plots full size airfoils of any desired chord length from a given set of coordinates. The first step of the structural design process was the use of AIRFOIL PLOT to obtain a full size template of the wing root chord. This template was used to determine the internal geometry of the wing. By using this

process, the location of items such as the front shear web, top and bottom spar caps, and housing tube was fixed (Figures 4 and 5).

Three inches was selected as the width of the top and bottom spar caps. The front shear web was inclined 1-1/2 degrees aft so that the wing will be mounted in the optimum position and the fuselage will provide the minimum drag during the cruise phase of flight. Once the geometry was determined the computer structural analysis was run. The program SPAR was used for this process. Initial inputs required were the vehicle gross weight less wing weight, load factor, wingspan, root chord, and tip chord. From this the program calculated the wing air load, shear load, and the bending moment. To size the spar, the program then requires the tensile or compressive strength of the cap, the shear strength of the shear web, the spar width, and the percent chord thickness. The program uses a factor of safety of two when calculating the ultimate design loads. From this input and the loads previously calculated the program calculates the spar height, cap thickness, and the web thickness. The program assumes the use of two shear webs; therefore the use of only one required that the value for web thickness be multiplied by two. The spar height is the distance between the centroid of the two spar caps. Once the final values are obtained, the computed spar height has to be compared to that of the actual spar height and adjustments made to the value of percent chord thickness until an exact agreement is obtained. For the initial inputs a value of ninety pounds was selected as the gross weight less wing weight. The wing was designed to a limit load factor of 4.4 g's (8.8 g's ultimate load). The value used for the wingspan was 11.5 feet and both the root chord and tip chord were 1.25 feet. Separate computations were required for the top and bottom spar caps since one is in tension and the other in compression during normal flight conditions.

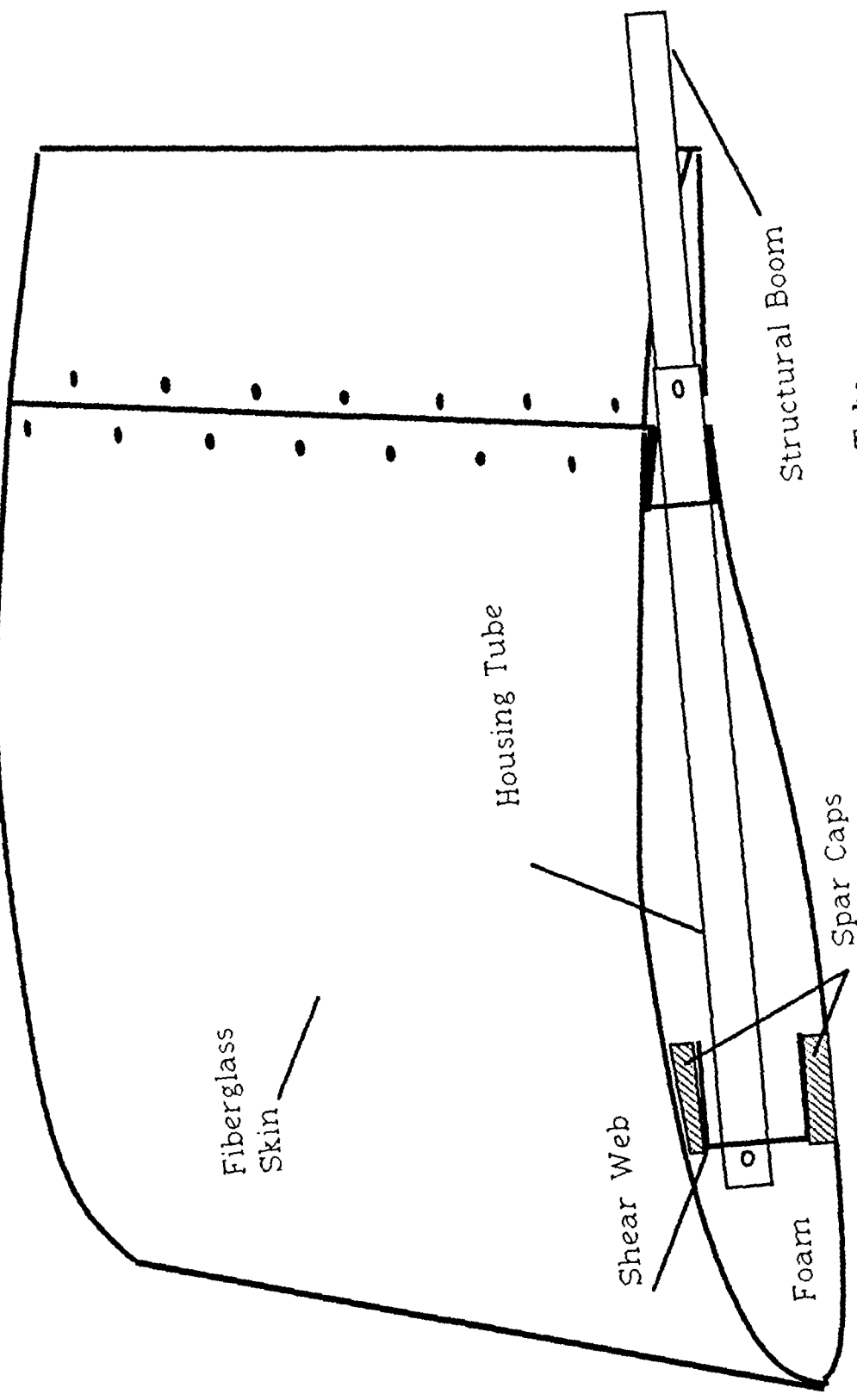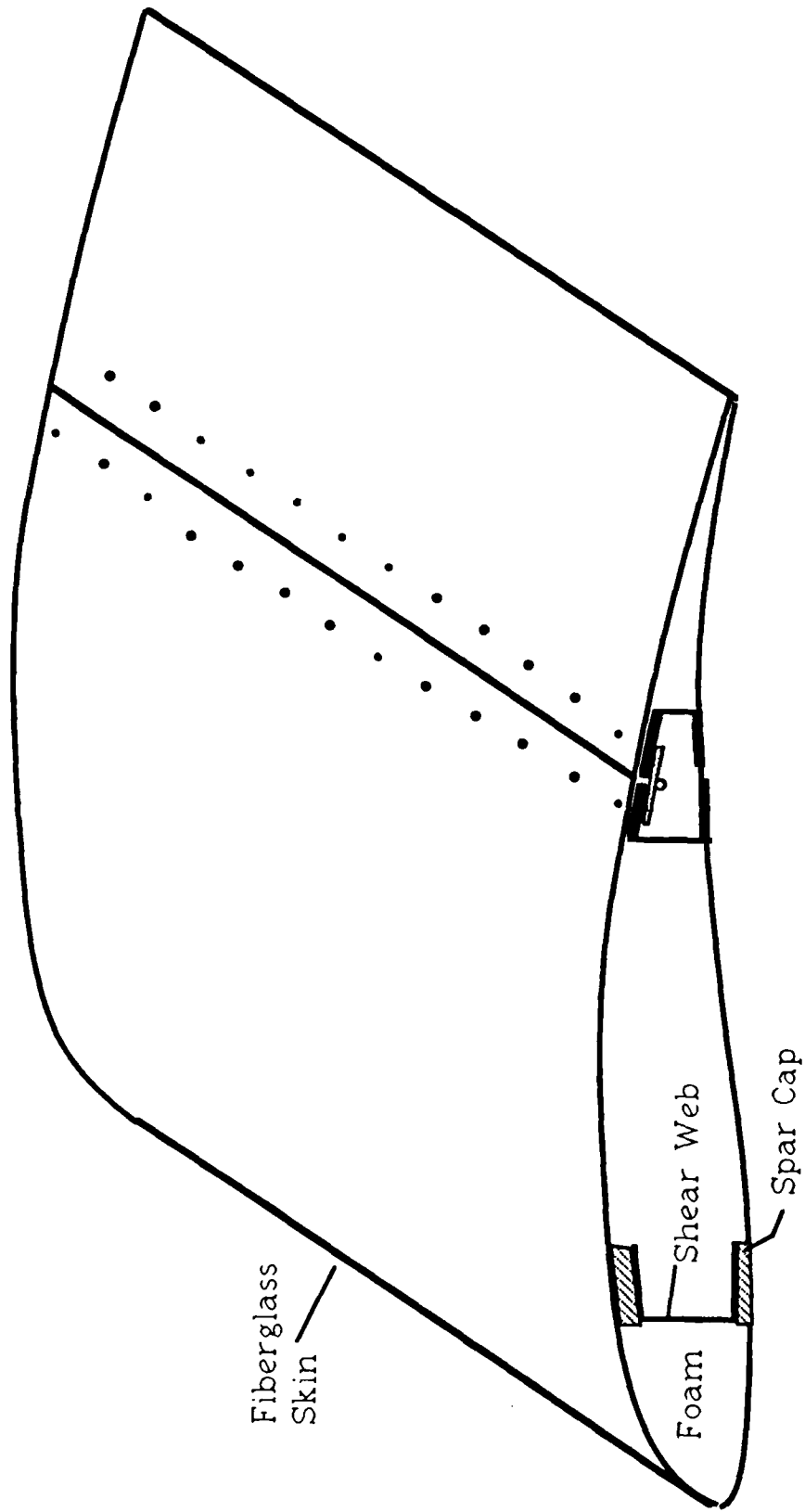**Figure 4. Wing Cross Section With Internal Housing Tube**

Structural Boom

Housing Tube

Spar Caps

Fiberglass Skin

Shear Web

Foam

30

Figure 5. Wing Cross Section Without Internal Housing Tube

Fiberglass
Skin

Foam

Shear Web

Spar Cap

RA 5177 Uni-directional fiberglass was used for both spar caps and it possesses ultimate tensile and compressive strengths of 66 and 43.5 ksi. respectively. RA 5277 Bi-directional fiberglass was used for the shear web and it has a shear modulus of 0.6 msi. The computer printout of this structural analysis is contained in Appendix B.

The wing spar box was designed in a manner analogous to that of the wing spar; however, a design limit load of 6 g's was used. The thickness calculated for the root of the spar caps was used throughout the entire span vice tapering the spar caps. Additionally, since two shear webs are employed, the shear web thickness does not have to be increased. Figure 6 shows the details of spar box construction. The results of the computer analysis are also contained in Appendix B.
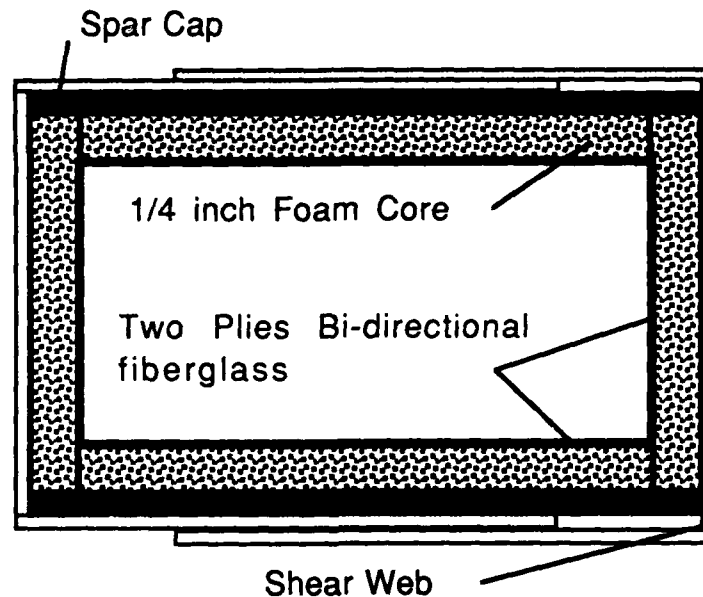

Figure 6. Spar Box Cross Section

3. Horizontal Tail Design

This design makes use of a single, rectangular platform, medium aspect ratio horizontal tail attached to the fuselage pod by two structural aluminum tubes as previously mentioned. An airfoil suitable for tail design will usually be of symmetrical section, and preferably no thicker than 12 percent of the chord length. Although the tendency would naturally be toward selection of a thicker section to reduce bending stresses, the airfoil section lift slope falls off rapidly above 12 percent thickness while, of course, the section drag increases. The lift curve slope of an airfoil is based upon the straight portion of the lift curve and is the ratio of lift coefficient increase per degree change in angle of attack. The higher the lift slope value the greater the tail lift and damping action, which in turn means increased longitudinal stability and control response. The airfoil selected for this surface was the symmetric NACA 0012 section. [Ref. 14:p. 94] It was necessary to compromise with a thicker airfoil section in order that most of the structural attachment housing could be contained within the confines of the airfoil surface.

Upon scaling the Pioneer's empennage, the chord for the horizontal tail was selected as 8.5 inches which appears to be in good proportion with that of the wing. While the planform design of the horizontal tail is frequently as much a matter of artistic effort or structural simplicity as aerodynamic consideration, tail aspect ratio should be as high as structural loading permits. This is generally around 3 to 4 for horizontal tail surfaces. [Ref. 14:p. 95] Reference 12, page 416, recommends that horizontal tail aspect ratio be approximately two-thirds that of the wing aspect ratio. For this design that would equate to an aspect ratio of 6.13. An average of these two guidelines was adopted and 5.5 was selected as the horizontal tail aspect ratio.

From the chord and aspect ratio, values for the span and area were calculated. The values obtained were 3.89 feet and 2.76 ft.^{2} respectively.

The primary requirement for longitudinal stability is adequate horizontal tail power. Horizontal tail power is a combination of horizontal tail area and the tail moment arm, the distance from the airplane center of gravity to the horizontal tail center of lift. The greater the tail arm the smaller the horizontal tail can be for the same moment, explaining why sailplanes have long tail arms and small tail surfaces to reduce both tail surface drag and control surface displacement drag. The longer the tail arm the more stable an airplane will feel and actually be in flight, due to the damping action provided by the horizontal tail. On the other hand when the tail arm is too short, any airplane will tend to become marginally stable longitudinally, and finally will become unstable in pitch as the center of gravity moves aft. The degree or level of positive longitudinal stability, which is a function of the tail arm in addition to the tail volume ratio, will steadily decrease as the center of gravity moves aft because the tail arm is decreasing while distance to the aerodynamic center is increasing. As a good first approximation, the one-third chord point of the horizontal tail should be located 2.75 to 3 times the wing mean aerodynamic chord (MAC) distance from the wing quarter chord point. [Ref. 14:p. 93] For this design that should equate to a value of 41.25 to 45 inches. Since the Pioneer RPV is considered to be deficient in tail power as alluded to earlier, to insure good longitudinal stability a conservative estimate of 52 inches was used as the design basis.

Reference 14, page 94, recommends that the horizontal tail power or horizontal tail volume coefficient be greater than 0.55 and Reference 12, page 395

recommends 0.3-0.65. Values of 0.648 to 0.666 were calculated for this RPV depending on which definition of tail arm was used.

A ratio of the horizontal tail area to wing area yields a value of 0.192 which falls within the guidelines of 0.16 to 0.20 [Ref. 12:p. 417].

The pitch control for this design is provided via a single simply hinged elevator which is a integral part of the horizontal tail. Guidelines for sizing the elevator suggest that the area ratio of elevator area to horizontal tail area should be between 0.5 to 0.55 [Ref 12:p. 417]. This horizontal tail has vertical fins attached on both outboard ends which reduces the area available for the elevator. This restriction necessitated that the elevator chord comprise over half of the horizontal tail chord. The dimensions selected for the elevator were 44.4 inches by 4.6 inches, which equates to 204.24 in.^{2} of area. The area ratio fell nicely within the guidelines at a value of 0.514.

Before a structural analysis of the horizontal tail could be conducted, the loads on the surface had to be determined. As per Reference 15, pages 38-47, two methods were used to calculate the loads, then the design was based upon the method that yielded the higher loading. The first method was in accordance with the design criteria contained in FAR Part 23. The tail load as determined by this method was 67.37 pounds of force. An additional benefit of this method is that certain airspeed limitations are obtained. The restrictions determined were the maximum flap speed (76.66 mph), maximum maneuvering speed (104.54 mph), maximum dive speed (167.27 mph), and the never exceed speed (178.49 mph). Method two makes use of a worst case condition, that is, with the aircraft loaded so that the c.g. is one foot forward of design location, airspeed at the never exceed speed, and the aircraft pulling up hard at the design limit load (4.4 g's). Moments are taken about the

quarter chord which allows the horizontal tail surface load to be determined. This method yielded a load of 178.78 pounds; therefore, the horizontal tail was designed to withstand a load of 180 pounds of force. The same methods used in the wing analysis was used for the horizontal tail and the results are contained in Appendix C.

The horizontal tail will be constructed using the same "moldless" composite construction technique outlined in the section on wing construction. Figures 7 and 8 show the details of a typical horizontal tail cross section.

4. Vertical Tail Design

A pair of identical vertical fins, each mounted on the outboard tip of the horizontal tail, provides the directional stability for this vehicle. The majority of the vertical fin area is mounted above the horizontal tail surface. The fin, a tapered planform, 15 inches in length or span, has a root chord of 8 1/2 inches which is reduced to 5 inches at the tip. A small segment of the vertical fin extends below the horizontal tail, to provide additional area for stabilization and to serve as an attitude limiter in the takeoff and landing modes thereby preventing damage to the propeller. Rudders, each measuring 4.6 inches x 11.5 inches, are incorporated within each vertical fin and by operating through a common linkage, provide the necessary yaw control.

The vertical fin must be sufficient to ensure that the aircraft will tend to remain in equilibrium at zero sideslip and the rudder must maintain zero sideslip during maneuvers that introduce moments tending to produce sideslip [Ref. 19:p. 315]. Vertical tail power is a primary design criterion for the vertical tail and provides a quantitative measure for determining the effectiveness of the
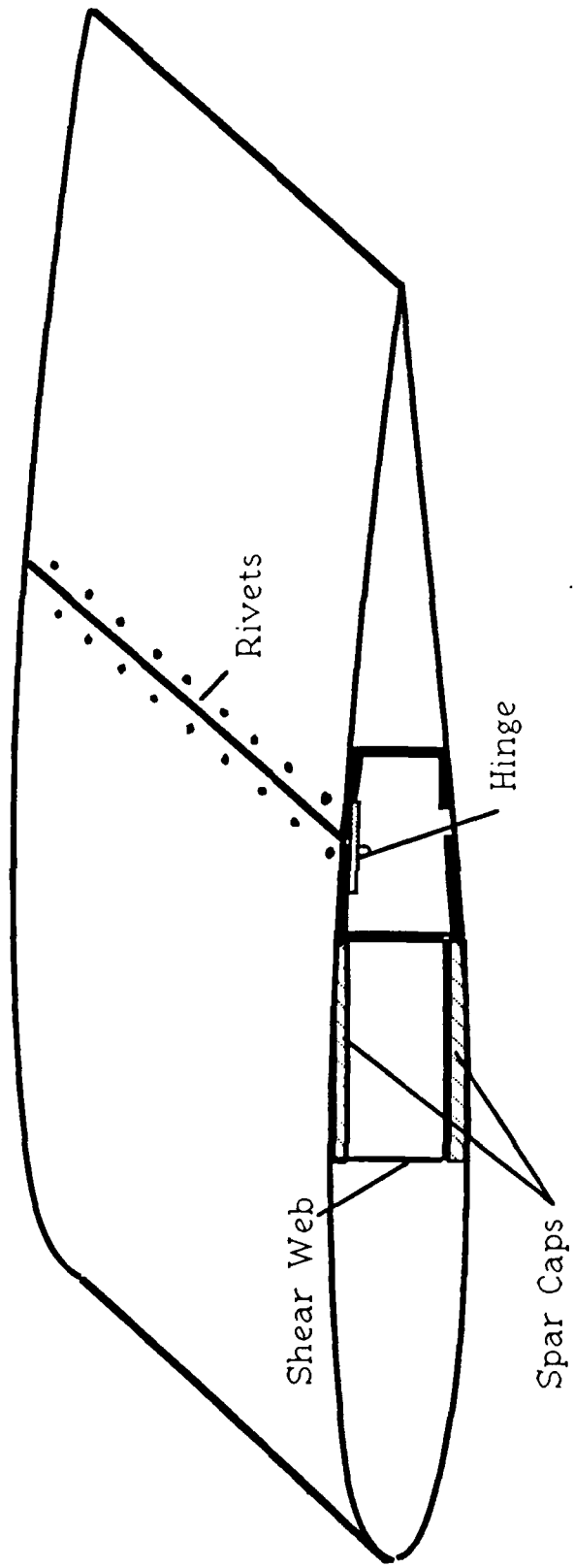
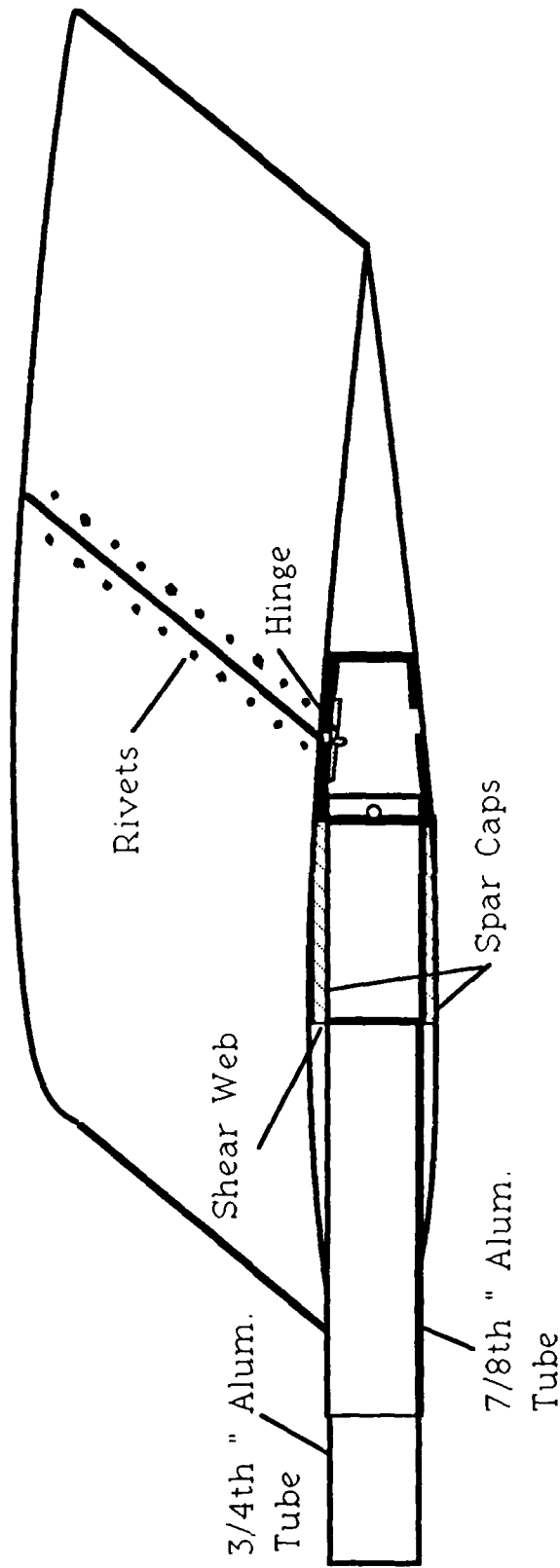**Figure 7. Horizontal Tail Without Internal Housing Tube**

Rivets

Hinge

Shear Web

Spar Caps

37

Figure 8. Horizontal Tail With Internal Housing Tube

Hinge

Rivets

Spar Caps

Shear Web

3/4th " Alum. Tube

7/8th " Alum. Tube

vertical tail and rudder design. Reference 14, page 94 suggest that to be effective, the vertical tail power should exceed an empirical value of 0.30. Using the dimensions previously mentioned, the vertical tail was found to contain 211.25 in.^{2} in overall area. Using this value and a vertical tail arm of 51.85 inches, the vertical tail volume or vertical tail power was found to be 0.3527, which exceeds that value necessary for adequate directional stability.

Further analysis of the vertical tail was conducted by examining the area ratio of the overall vertical tail area to that of the wing. This value (0.102) was found to be larger than the 0.075 to 0.085 range suggested by Reference 12, page 417. However, the larger than necessary area was retained to ensure directional stability due to the large amount of fuselage area forward of the center of gravity which acts to destabilize the aircraft in yaw and the possibility that even more destabilizing area will be generated in the future, should external flight research equipment be added. The ratio of area of the rudders (105.8 in.^{2}),when compared with that of the total vertical fin area was found to be 0.5. This value is within the guidelines of 0.5 to 0.6 [Ref. 12:p. 417].

To be effective aerodynamically and still remain within structural weight limitations, all modern tail surfaces are of fairly thin section and relatively low aspect ratio. The NACA 0009 airfoil, commonly used for tail surfaces, especially in situations in which a minimum of internal structure is required, was selected for the vertical fins. An aspect ratio of around 2 to 3 is generally adequate for vertical surfaces [Ref. 11:p. 208 and Ref. 14:p. 94]. Analysis of this design yields approximately 2.13 for the vertical tail aspect ratio.

The fiberglass and foam composite structure of the vertical tails and rudders is similar to the structure of the horizontal tail and elevator; however, no

shear web or spar caps are incorporated. Each vertical fin will be bonded directly to the horizontal surface and with the aid of fiberglass reinforcement, become a permanent part of the horizontal tail. Additional details on the actual construction process are contained within the section describing vertical tail construction.

5. Landing Gear Design

The landing gear arrangement used on RPVs is quite diverse and depends primarily upon the proposed operational environment. For the Pioneer, the design upon which this study was based, the operational environment is primarily the deck of a battleship. Operation from this platform does not require the use of a landing gear system, for the vehicle is launched from a launcher rail using jet-assisted takeoff (JATO) and recovered by flying into a net. Only when being operated from a shore-based facility is the vehicle fitted with landing gear.

This RPV design is expected to operate only from shore-based facilities using both improved and unimproved runway surfaces. This environment requires a landing gear system that is both rugged and easy to maintain. The use of a pusher engine dictated that a tricycle arrangement be utilized. For simplicity and ruggedness a solid slab spring gear was selected for the main landing gear. This design was popular on general aviation aircraft in the 1940's and 50's. This arrangement is unique in that no shock absorbing or oleo system is required because the dimensions of the slab material can be altered to provide the required "springyness".

Using a static taildown angle of 15 degrees, a tipback angle of 20 degrees, and an overturn angle of 45.5 degrees, the landing gear was laid out in accordance with Reference 13, page SAWL-5, the results of which can be seen in Figure 9. The main gear axle centerline is located 47.65 inches aft of the nose or 6.95 inches from

the forward face of the firewall. The nose gear axle centerline is located 9.0 inches aft of the nose or 45.6 inches from the forward face of the firewall. Located in this position the main gear supports 87 percent of the aircraft weight (104.4 lbs.) while the nose gear supports the remaining 13 percent of the weight (15.6 lbs.).

With the engine mounted on the rear of the fuselage it is very important that the main gear be designed so as to not allow the propeller to strike the ground in the takeoff or landing phases of flight. The landing phase was used to govern the design because the aircraft will normally be subjected to greater than one g load upon landing and it is at this position that clearance will be most critical. It was determined that the aircraft could attain a nose up attitude of 15 degrees before striking the lower portion of the vertical fins. Utilizing a 20 inch diameter propeller, a rotation to this attitude will result in approximately one inch ground clearance for the propeller.

Using the procedures outlined on page 225 of Reference 14, the main wheel and strut were designed to absorb a two g impact and still provide sufficient propeller clearance. The base dimension and thickness of the strut as well as material used were altered to achieve satisfactory performance. The result is that the gear shall be manufactured of 5/16th inch thick 2024 aluminum with the base dimension being 4 1/2 inches. This design will allow 0.98 inches of deflection following a two g impact. It is recommended for added protection, that wire runners be attached to the bottom of both vertical fins so as to limit the rotation attitude to less than 15 degrees.
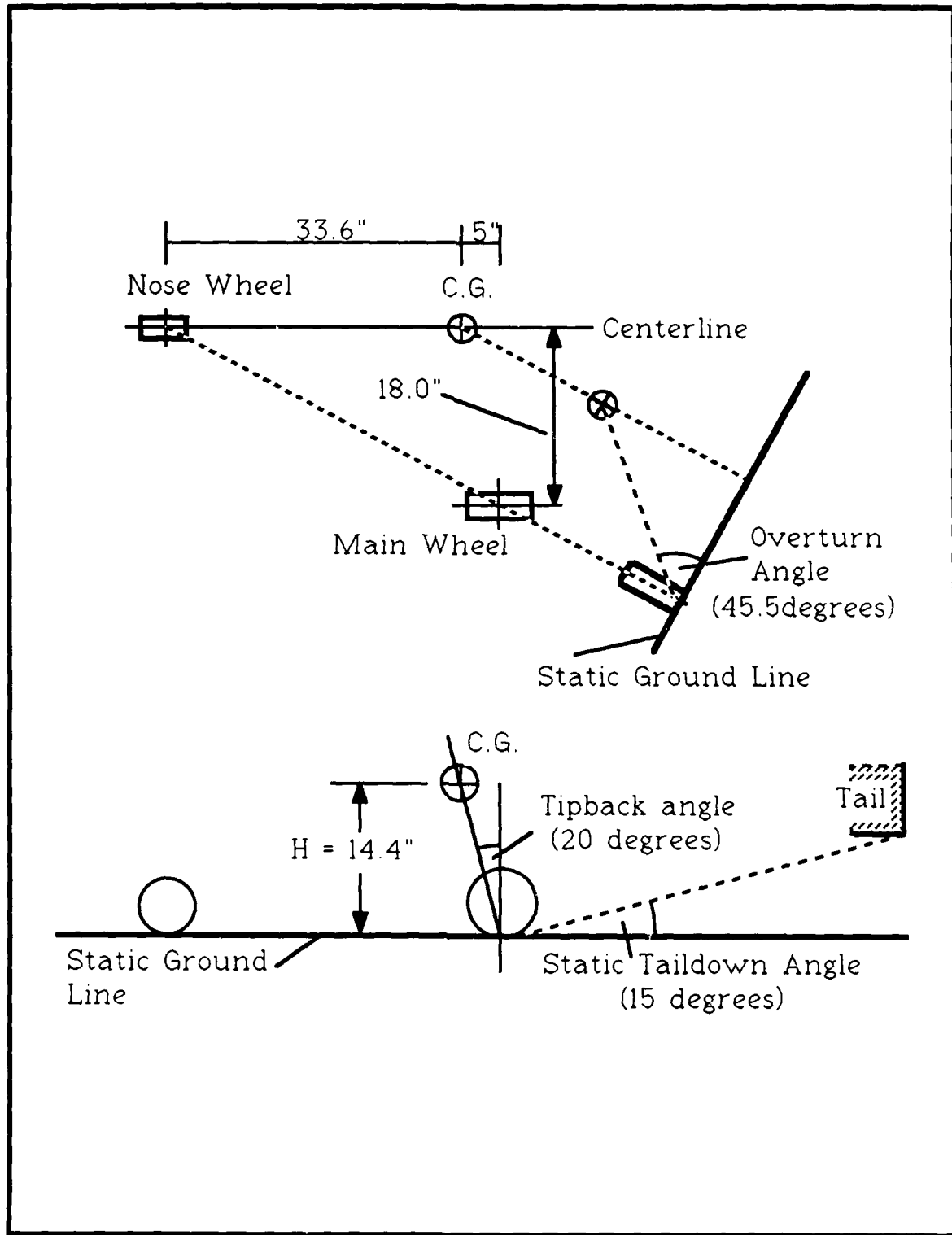
41

Figure 9. Landing Gear Geometry

The gear strut, which looks like a cone when viewed from the side, gradually tapers to a width of 2 inches at the point where the axles attach. The axles, which bolt to the strut using four 3/16-inch diameter bolts, were designed to fit the four-inch diameter "Azusalite" nylon wheels previously procured. The axles will be machined out of a solid billet of 2024 T3 aluminum. All landing gear manufacturing will either be accomplished by a machinist at the Naval Postgraduate School or contracted with an outside agency. This strut/wheel combination provides for a wheelbase of 36 inches measured between the two wheel centerlines. With the incorporation of a pair of 2.80/2.50-4 pneumatic main tires the bottom of the aircraft will rest approximately 10.25 inches above the ground.

The nosegear consists of a six-inch diameter wheel mounted between a C-section shaped housing formed out of 1/8th inch aluminum sheet. The housing is attached to the fuselage by a 3/4th inch diameter aluminum tube bent into the shape of an inverted question mark as shown in Figures 2 and 10. The C-section housing is secured to the tubing by an arrangement of spacers, bolts and conduit pipe clamps. The other end is mounted within the fuselage using two phenolic bearing blocks which allow for easy rotation. A locking pin or bolt, used in conjunction with a series of large flat washers approximately 1-1/2 inches in diameter mounted on the bottom of the fuselage and on the top phenolic block, prevent excessive vertical movement of the nosegear strut.

The rudders do not become an effective means of directional control until sufficient airspeed is attained; therefore, some method of control must be provided for ground taxi and takeoff operations. A control horn or bellcrank, of sufficient length to provide maximum mechanical advantage, is bolted to the aluminum tube

strut between the two bearing blocks. An onboard servo connected to the control horn will allow for external directional control.

A spring, which slips over the outside of the aluminum tube strut and is located between the two flat washers on the bottom of the fuselage will act to absorb the landing shock transferred to the nosewheel. Figure 10 is included to help clarify the nosegear design and the method of attachment.

6. Engine /Propeller System

Propulsion systems for RPV applications require a high thrust-to-weight ratio, good specific fuel consumption, and proven reliability. Some additional items considered when determining the engine to use for this design were size, cost, fuel used, type of cooling, and the number of cylinders.

The initial power estimate was that approximately twelve horsepower would be require to safely operate this design. In addition to this, it was mandatory that the engine size and weight be minimal. As a flight research vehicle, specific fuel consumption was not a driving factor because many hours of on station or loiter time are not required. It was estimated that most flights would be one hour or less in duration. Due to the fact that there is only one vehicle being constructed from this design, the engine selected had to have a proven track record of reliable performance. This program cannot suffer the loss of an air vehicle and all the related avionics due to an engine related malfunction. Additionally, the cost incurred in procuring the engine has to be reflective of the benefits the RPV will provide and should also be in cost proportion to the airframe and avionic systems. It was also a requirement that either aviation or automotive fuel be used to operate the engine to alleviate the cost and procurement problems associated with the use of
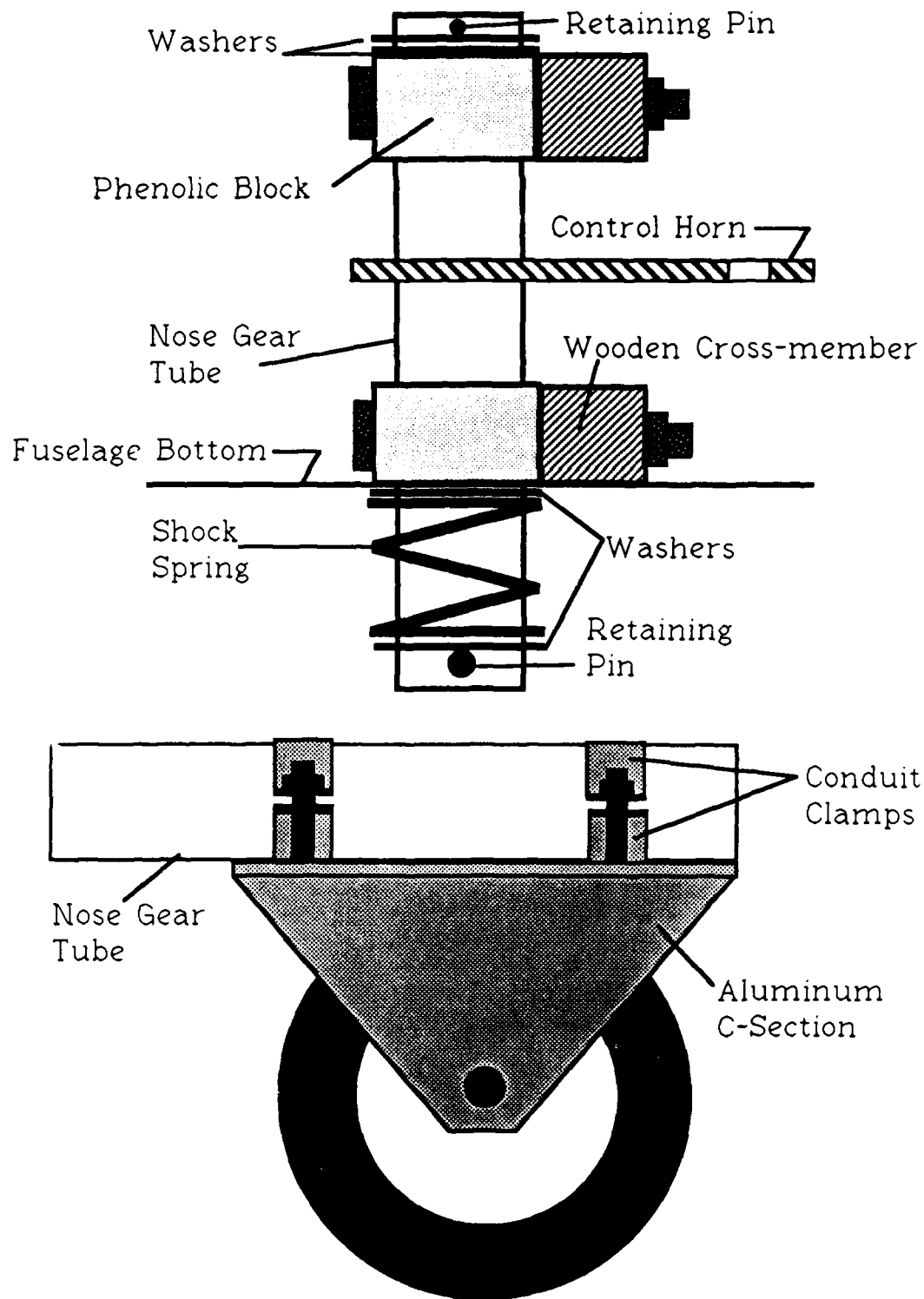
Figure 10. NoseGear Upper and Lower Attachment Detail

alcohol based fuels such as those used by the modeling community. Any water cooled engines were ruled out due to the added weight and complexity that such a cooling system would add to the RPV. An engine with two or more cylinders was desired in an attempt to minimize the vibration transmitted to the airframe and avionic systems.

The engine selected which most closely satisfies all these requirements was the Limbach L275 E manufactured by Limbach Flugmotoren of West Germany and distributed by Limbach Aircraft Engines of Tulsa, Oklahoma (Figure 11).

According to the company's sales brochure, the Limbach L275 E, designed to operate on 90 octane fuel mixed with a suitable SAE 30 two-cycle oil is an aircooled, two cylinder, horizontally opposed, two cycle engine, developing 20-25 horsepower at 7300 rpm. The engine is roughly 15 1/2 inches wide, 7 1/2 inches long, 7 3/4 inches tall and weighs 16 1/2 pounds. It is one of the few small RPV engine to have been combat proven. The Israeli military have used the L275 E engine to power the MASTIFF UAV for many years.

The engine can be adapted to the fuselage using several methods; however, the most promising technique is to bolt the engine directly to the firewall using Lord mounts or other similar vibration damping devices. Structural reinforcement will need to be added to the forward face of the firewall, especially in the areas where the bolts pass through. The structural reinforcement was not installed during fuselage construction because the actual engine was not in hand and the designer did not have exact dimensions of the mounting flanges. Whatever
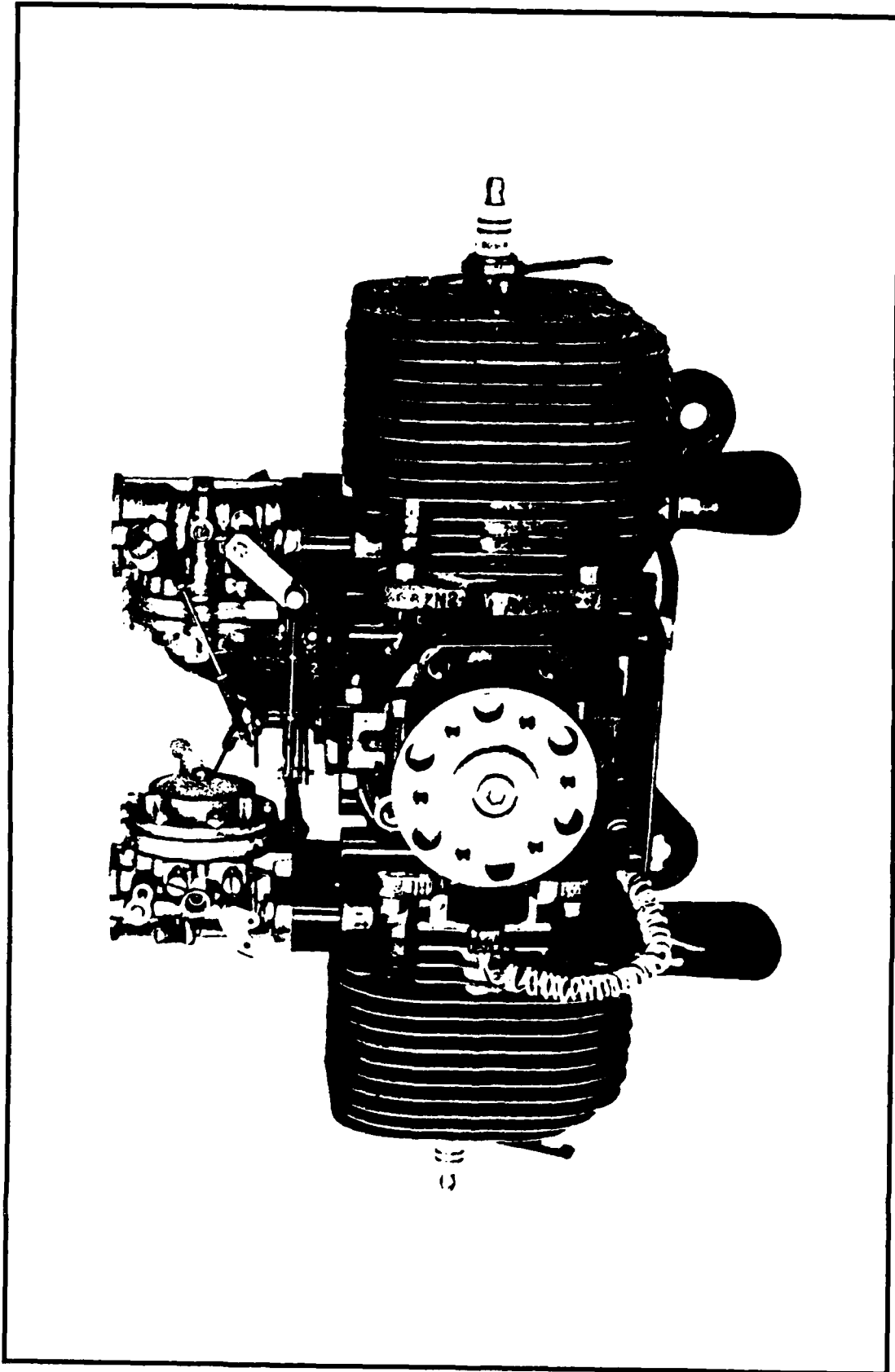
Figure 11. Limbach L 275E RPV Engine

method is ultimately used to mount the engine, it will be necessary to ensure that the engine centerline is mounted one inch below the fuselage centerline as indicated in the aircraft design drawings.to provide adequate clearance between the engine and cowling. Additionally, to enhance the airflow through the propeller, the engine will require an extension approximately two inches in length between the crankshaft hub and the propeller in an attempt to give sufficient length to the engine cowling so that it can be reduced from the large oval shape at the firewall to an oval shape approximately 11 1/2 inches wide and 5 3/4 inches tall at the propeller hub.

No specific propeller has been selected for the design as of this writing. The only restriction so far in the design is that the propeller diameter should be limited to twenty inches or less. This restriction is to ensure proper propeller to ground clearance. After the exact horsepower required has been determined, detailed power available charts for the L275E will be obtained and the operating rpm for this design determined. Only after this information is in hand, can a logical choice for propeller pitch be made. A standard propeller, as used on a small ultralight, might prove feasible, but it is most likely that it will have to be custom made. Whatever propeller is selected, it should be manufactured of wood to better absorb the pulsing dynamic load imposed due to an asymmetric cowling. Furthermore, it should have some form of leading edge protection. This is most critical for pusher designs because any debris that falls off the aircraft will pass through the propeller disk.

V. AIR VEHICLE STABILITY

Satisfactory performance as a trainer and flight research vehicle require that the air vehicle be stable, especially in the longitudinal mode. A stability analysis was conducted for the longitudinal and directional modes. The equations used for stability calculations are contained in Appendix A.

A. LONGITUDINAL BALANCE AND STATIC STABILITY

Some requirements for longitudinal static stability are that: (1) $C_{M\alpha}$ must be negative, (2) C_{Mo} must be positive, (3) the position of the center of gravity must always be forward of the neutral point, and (4) the static margin, which is a measure of the longitudinal static stability, must be positive. The larger the static margin, the more stable the aircraft.

Equation #1 is required for the calculation of $C_{M\alpha}$. Analysis of this equation indicates that many of the variables are unknown and need to be calculated. The first variables approached were the lift-curve slopes of the wing and horizontal tail. Before these values could be examined it was necessary to estimate the Reynolds number that each of these surfaces would be operating at during the majority of the RPV's mission. Using Equation #2 and 75 miles per hour as the design cruise speed, it was determined that the wing would be operating at a Reynolds number of approximately 8.745×10^5 and the horizontal tail at 5.033×10^5 during cruise. With these data at hand the proper lift curves were selected. The Wortmann FX63-137 airfoil lift curve data corresponding to a Reynolds number of 7.0×10^5 were the closest to the calculated Reynolds number and therefore selected for the calculation of the wing lift slope. The NACA 0012 airfoil lift curve

corresponding to a Reynolds number of 3.0 x 10 [6] was selected for the calculation of the horizontal tail lift slope since this was the lowest Reynolds number for which data were available [Ref.17:p A-368]. Using values from the lift curves and Equation #3 the two-dimensional lift-curve slopes of 0.1088 and 0.1054 per degree were determined for the wing and horizontal tail respectively. For stability calculation purposes it was necessary to convert the lift-curve slopes from two-dimensional to three-dimensional values. This was accomplished using Equation #4. The three-dimensional lift-curve slope was determined to be 0.0809 per degree for the wing and 0.068 per degree for the horizontal tail.

The next variable calculated was the angle of zero lift for the wing. This value is the same for finite and infinite wings and is used to convert the angle of attack into an absolute measurement. Rearrangement of Equation #3 allowed for the calculation of this value. The angle of zero lift was found to be -7.97 degrees (measured from the zero lift line to the chord line).

The $\partial\varepsilon/\partial\alpha$ was calculated using Equation #5. The data used in this formula were obtained from the section on wing design. The value determined for this variable was 0.3133.

$(C_M)_{fuselage}$, which is the affect the fuselage has on the longitudinal stability, was calculated as a constant (0.01635) times the absolute angle of attack. It was found by using Equation #6.

The values of h (c.g. location), h_{ac} (aerodynamic center location), and V_H (horizontal tail volume coefficient) were obtained from the wing design section and are 0.30 chord, 0.25 chord, and 0.648 respectively.

$(C_M)_{ac}$ was calculated by converting the two-dimensional moment coefficients for the Wortmann FX63-137 airfoil [Ref. 20:p. 79] into three-dimensional

50

coefficients using Equation #7. The three-dimensional moment coefficients were correlated to an absolute angle of attack vice geometric angle of attack to provide continuity in Equation #1.

Next it was necessary to determine the downwash angle (ε_o) at the tail when the wing-body combination is at zero lift. Reference 16, page 363, states that this value is usually obtained from wind tunnel data; however, the iterative process described below was used. Using the design speed of 75 miles per hour (110 ft/sec) and Equation #8 the required C_L for the trimmed condition was determined as 0.58. With the use of this value and the wing three-dimensional lift curves it was found that the wing will achieve this value at an absolute angle of attack of +6.45 degrees (-1.52 degrees geometric). At this point, various values were substituted into Equation #1 for the combined bracketed terms i_t and ε_o until the value was obtained whereby $(C_M)_{cg}$ was equal to zero at + 6.45 degrees absolute. This was found to occur when the term $i_t + \varepsilon_o$ was equal to 6.1 degrees (Figure 12). To perform the iterative process it was initially assumed that i_t was equal to 5.5 degrees and ε_o was equal to 0.60 degrees. A sketch was made of the aircraft with a horizontal reference line representing the fuselage upon which the wing and horizontal tail were drawn at their respective absolute values. The zero reference line was then varied in angle of attack. At each point, the new absolute angles of the wing and horizontal tail were determined and multiplied times the respective component lift curve slope, thereby obtaining C_L for each surface. The C_L value was multiplied by the dynamic pressure to obtain values of lift created by the wing and horizontal tail. This process was repeated until the values for lift were equal and opposite. This was found to occur at an aircraft angle of attack of -4.8 degrees. This value of AOA and the associated wing C_L value of 0.1335 correspond to the

zero lift condition. This value of C_L was substituted in Equation #9 to determine the actual ε_o at the zero lift condition, which was found to be 0.53 degrees. The entire process was repeated again using $\varepsilon_o = 0.53$ degrees and $i_t = 5.57$ degrees. This iteration produced a value of -4.78 degrees as the zero reference angle of attack, a wing C_L of 0.1351, and an ε_o value of 0.536.

From this process it was determined to fix the tail setting angle at 5.57 degrees as measured counter-clockwise from the zero reference line to the horizontal tail leading edge chord line. It should be noted here that a change in horizontal stabilizer incidence angle i_t in no way changes the slope of the stability curve and therefore has no effect on the basic stability of the airplane. The only effect of variation in stabilizer incidence is a shift of the trim point [Ref 21:p. 434].

The next requirement for stability is that the $\partial(C_M)_{cg} / \partial\alpha$ must be negative. Using Equation #10 this value was found to be -0.02621. Observation of Figure 12 will also confirm that this value is indeed negative.

Equation #11 was used to locate the stick fixed neutral point. It was found to lie at 0.624 chord. Since the c.g. is located at 0.3 chord, the third longitudinal stability requirement that the c.g. must lie forward of the neutral point is satisfied.

As a measure of this stability, the static margin was calculated using Equation #10. The static margin was found to be 0.324 chord.

B. DIRECTIONAL STABILITY

The problem of directional stability and control is first to ensure that the airplane will tend to remain in equilibrium at zero sideslip and second to provide a control to maintain zero sideslip during maneuvers that introduce moments tending to produce sideslip [Ref. 19:p. 315].

The directional stability of the airplane can be assessed if a curve of yawing moment coefficient, C_n, with angle of sideslip, β, is obtained for any given aircraft. A positive slope of this curve is required for static directional stability. The derivative $dC_n/d\beta$ will be given in the short hand notation $C_{n\beta}$, and will be given per degree. [Ref. 19:p. 317]

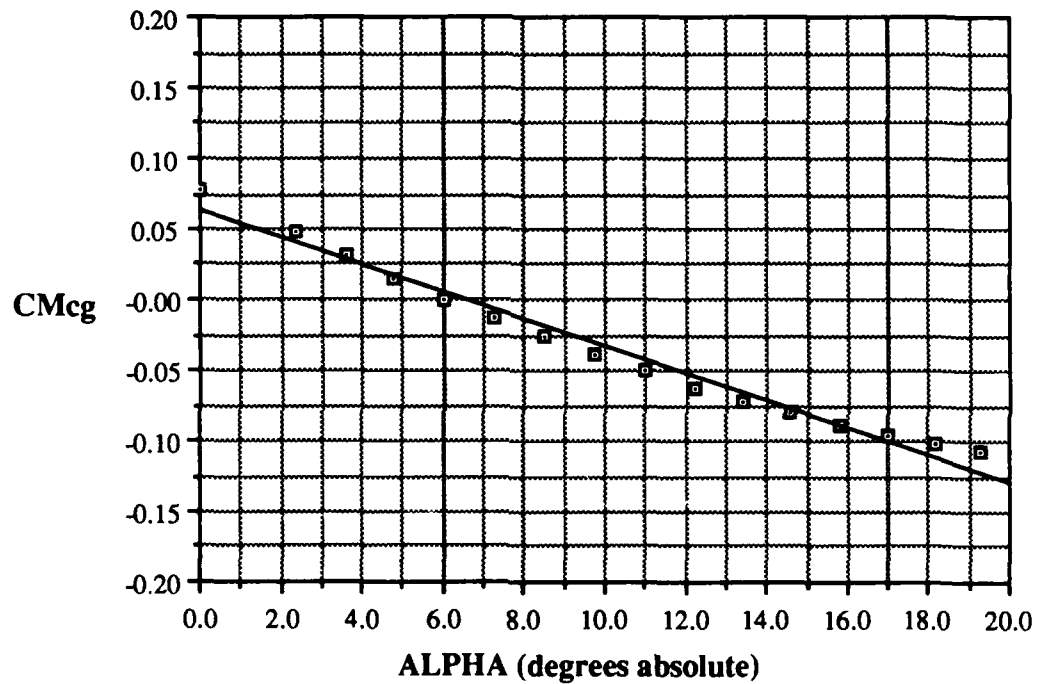**Figure 12. C_M cg versus α with i $_t$ + ϵ $_o$ = 6.1**

It should be noted that the reference cited above defines this directional stability derivative and the associated sign convention with respect to angle of yaw, Ψ. Current practice is to define the derivative with respect to β and sign convention as +β if the airflow is approaching from the right side of the aircraft.

The final directional stability derivative is comprised of contributions from many parts of the airplane. In order to obtain this derivative, the magnitude of the contributions from the major components must be developed analytically and then summed up. [Ref. 19:p. 317]

The first major component analyzed was the wing. The contribution of the wing to the airplane's directional stability is very small, with the angle of sweepback being the primary factor. The stability contribution of straight wings is almost negligible in comparison to the contributions of the other parts of the airplane [Ref. 19:p. 318]. The wing contribution was found to be zero for this design using Equation #13 since the quarter chord has no sweepback.

The contribution of the fuselage to the directional stability of the airplane is usually unstable and certainly one of the major effects. For normal airplane configurations this value varies from -.0006 to -.0012 [Ref. 19:p. 319]. Equation #14, developed by the North American Aviation Company during World War II, was used to calculate the value for this design. The value calculated was -0.00139 which is slightly higher than the maximum of the range indicated above. This is probably due to the fact that the suggested range is for normal aircraft configurations and with this design being a pusher, it has most of the fuselage forward of the c.g., which is destabilizing.

The directional stability of the combination of wing plus fuselage is usually slightly different from the sum of the two components obtained separately. This is due to the interference flow created at the wing-fuselage juncture. This interference effect is usually slightly stabilizing, but the contribution is never much larger than $\Delta C_{n\beta} = +.0002$ and in this case was +.0001 for the midwing design. [Ref. 19:p. 320]

For some designs, a running propeller can have large effects on the airplane's directional stability. Although stabilizing, the magnitude of the contribution for this design is almost neglible. This value was found to be +0.00004 for a windmilling propeller by using Equation #15. According to Reference 19, page 322, the contribution at full power is simply one and one-half times the value obtained for a windmilling propeller. This equates to a value of +0.00006.

The vertical tail is the additional stabilizing surface that must be incorporated to overcome the instability of the other parts of the aircraft and to give the desired level of directional stability [Ref. 19:p. 322]. Equation #16 was used to calculated the two-part contribution of the vertical tail. $(C_{n\beta})_v$, the primary directional contribution of the vertical tail which is a function of vertical tail lift curve slope, volume coefficient, and tail efficiency was found to be equal to +0.00222 and $\Delta_2 C_{n\beta}$, which arises from the sidewash or interference flow from the wing-fuselage combination, was found to equal to -0.0001.

The directional stability derivative for the aircraft $C_{n\beta}$ was determined by summing the contribution of all the major components as calculated above. The derivative was found to equal +0.00109 at full power and +0.00074 with the propeller windmilling.

A desirable value of +0.00048 for $C_{n\beta}$ was obtained from Equation #17. Therefore, this design should exhibit good directional stability in both the power on and power off conditions of flight.

VI. CONSTRUCTION TECHNIQUES

The perfect airplane should have every component devoted to smooth aerodynamics and structural strength. The ideal way to make the complex curvaceous shapes of airplanes has finally come about by the use of plastic resins combined with very strong fibers. Composite construction is unique in that form and function are both achieved within the same component, something that has been a design goal for many years.

The West Germans pioneered plastic construction when they made the Phoenix sailplane almost entirely of fiberglass. Now, most of the top sailplanes are German and made of composite plastic. [Ref. 22:p. 10]

In the United States, fiberglass was first used in less stressed parts, such as wing tips and fairings. But now, composites are used for major structures. Sometimes a foam or balsa wood core is covered with fiberglass on each side, making a much stiffer part. Steel or aluminum fittings can be fastened into the composite as "hard points" to transfer loads. High strength carbon fibers and Kevlar cloths and filaments are available to make structures that reach undreamed-of perfection, both structurally and aerodynamically. [Ref. 22:pp. 6-10]

Several techniques of composite construction, primarily used in the construction of homebuilt aircraft, were used for the fabrication of this design. As individual components are discussed, each method used will be described.

A. FUSELAGE CONSTRUCTION

The fuselage was constructed using a method developed by the late Ken Rand which has found limited use throughout the homebuilt aircraft industry. Even

though this method will produce a heavier structure than the "moldless" construction technique to be used on the wing and empennage, it is desirable for the fuselage because the inner structure of plywood sheet and wood longerons facilitate the mounting of the avionic equipment without the installation of many hardpoint inserts or mounting pads that would be required if the latter technique were used.

In this method, the rectangular shape of the fuselage side was cut out of 1/8 inch thick aircraft plywood, after which 5/8 inch x 5/8 inch Douglas Fir longerons and support braces were glued to the plywood using "Weldwood" resorcinol glue. The same procedure was repeated for the reverse side, top, and bottom of the fuselage. At this point the four assemblies were joined to provide a box-like structure with a removable lid. This assembly is used to support the primary applied loads.

Templates made of 1/8th inch thick aircraft plywood, corresponding to the desired fuselage contour, were attached approximately every six inches along the length of the fuselage. The area between the templates was filled with blocks of urethane foam. The foam was then carved/sanded down to match the templates after which three plies of fiberglass was applied. Two different types of fiberglass and an epoxy resin matrix were used in this "skinning" process. The first layer, oriented the length of the fuselage, was uni-directional fiberglass which exhibits strength only in one direction. A second layer of uni-directional fiberglass was "layed up" in the area where the spar box exits the fuselage. The third layer which covered the entire fuselage was bi-directional fiberglass. This glass is easier to form over compound curves and exhibits approximately equal strength in all directions.

57

The foam and glass/epoxy network of this method is not the primary load carrier, but serves to provide aerodynamically favorable compound curves which cannot be achieved using metal or wood and a surface that cannot be rivaled for its beauty or durability. A sketch of a typical fuselage cross-section can be viewed in Figure 3.

B. WING / SPAR BOX CONSTRUCTION

The wing was constructed using a method pioneered by aircraft designer Burt Rutan. The method known as "moldless" composite construction is used to construct many of the popular homebuilt aircraft flying today, including the Rutan Long-Ez. The flying surfaces are built from the inside out, whereby cores for the airfoils are hot-wired out of a billet of styrofoam. The foam serves as the ribs typically used in conventional construction. If necessary, fiberglass and/or carbon fiber shear webs and sparcaps are layed up within the foam core and the core is faced with several plies of glass. A unique property of the glass/epoxy matrix is that it can be oriented any direction to supply the necessary strength. Composite "tailoring" allows different weave patterns, weave orientation, and even different types of glass and epoxy to be used depending whether the applied load is bending or torsional in nature. Components constructed in this manner are not susceptible to corrosion and provide a marked improvement in structural reliability over aluminum, steel or wood. An additional benefit is that the composite wing will not suffer a performance loss due to the airfoil contour deforming and wrinkling under load. [Ref. 23:p. 90]

Even though the wings are not under construction as of this writing, an attempt will be made to describe the anticipated construction sequence. The first step is to make several full-size plots of the FX63-137 airfoil using AIRFOIL PLOT. The

templates are used to provide the contour of the airfoil surface during the hot-wiring process. One set of smooth templates should be made and one set with the proper spar cap cutouts should also be made. All templates should be mounted together when drilling the mounting holes through them. Once satisfactory templates have been made, the smooth ones should be attached, with nails, to foam billets which have previously been hot-wired to the correct dimensions. The templates will allow smooth full-size foam cores to be cut for the wing. Next, the templates with the cutouts are attached and the spar cap cutouts made.The location of the shear web should be marked with special attention being paid to the fact that it is not vertical , but tilted aft 1-1/2 degrees. Now the front "D" section is hot-wired and removed from the wing core. The aileron/flap hinge line is now located and the aft portion of the wing is also hot-wired off. At this point the wing will be jigged in the vertical position, high density inserts installed and the shear web layed up. The shear web will consist of plies of RA 5277 Bi-directional fiberglass with the warp direction at ± 45 degrees to the longitudinal axis of the spar. Peel Ply will be used on the forward face of the shear web to assure proper adhesion when the "D" section is replaced and between the shear web and the spar caps. When the shear web has cured, the 7/8th inch hole for the horizontal tail attachment housing will be cut. The " D " section, except for the inboard eight inches, can now be reattached to the front of the airfoil and the previously removed aileron /flap sections can be reattached to the rear of the airfoil in those locations where appropriate. The spar caps are now fabricated using RA 5177 Uni-directional fiberglass with the primary fiber direction running the length of the spar. Peel Ply will be used on the top surface of the spar caps so that a good bond will be achieved between the spar caps and the wing skin. Now the two plies of bi-directional fiberglass are layed up on

59

both sides of the airfoil. After the airfoil skin has cured, the aileron and flap cutouts will be made and the exposed foam closed out as shown in Figures 3 and 4. At this point, the airfoil and flap surfaces can be hinged and the housing tube epoxied into place. An inspection panel or some other means will have to be incorporated so that the retaining pin can be installed in the forward edge of the housing tube. The inboard eight inches of the airfoil aft of the spar caps is now removed, high density inserts installed and the aft face of the spar glassed with plies of bi-directional glass to provide the box-like structure which slides into and is retained within the spar box.

The spar box is a relatively simple structure to fabricate. The four rectangular pieces are cut out of 1/4th inch foam and then glassed on one side with two plies of bi-directional glass oriented at ±45 degrees to the long dimension. The four pieces are then assembled as shown in Figure 6, insuring the unglassed surface is placed outward. The top and bottom spar caps are now fabricated and covered with Peel Ply. After cure, the Peel Ply is removed,the corners rounded and the shear webs layed up making sure to provide the proper overlap. When all fiberglass has cured, the wings will be positioned in the sparbox and retaining bolt holes drilled through the high density inserts and the spar box will then be installed into the fuselage.

C. HORIZONTAL TAIL CONSTRUCTION

The construction of the horizontal tail is almost identical to the procedure outlined for the wing. As with the wing, the first step is to make several full-size plots of the NACA-0009 airfoil using AIRFOIL PLOT. The steps employed prior to the cutting of the shear web are identical to those for the wing. The location of the shear web should be marked with special attention being paid to the fact that it is not vertical , but tilted forward 1/2 degree. Now the front "D" section is hot-wired and

removed from the wing core. The elevator hinge line is now located and the aft portion of the airfoil is also hot-wired off. At this point the surface will be jigged in the vertical position, high density inserts installed and the shear web layed up. The shear web will consist of plies of RA 5277 Bi-directional fiberglass with the warp direction at ± 45 degrees to the longitudinal axis of the spar. Peel Ply will be used on the forward face of the shear web to assure proper adhesion when the "D" section is replaced and between the shear web and the spar caps. When the shear web has cured, the 7/8th inch hole for the horizontal tail attachment housing will be cut. The entire "D" section, except for that small area around the housing tube, can now be reattached to the front of the airfoil and the previously removed elevator section can be reattached to the rear of the airfoil. The spar caps are now fabricated using RA 5177 Uni-directional fiberglass with the primary fiber direction running the length of the spar. Peel Ply will be used on the top surface of the spar caps so that a good bond will be achieved between the spar caps and the wing skin. Now the two plies of bi-directional fiberglass are layed up on both sides of the airfoil. After the airfoil skin has cured, the elevator cutout will be made and the exposed foam closed out as shown in Figures 7 and 8. At this point, the elevator can be hinged and the housing tube epoxied into place. When cured, the structural booms can be inserted into the wing and horizontal tail, thereby attaching the empennage to the fuselage.

D. VERTICAL TAIL CONSTRUCTION

Vertical tail construction is virtually identical to the methods used on the wing and horizontal tail except there will be no internal shear web are spar caps. The vertical tails are simply hot-wired from foam billets using NACA 0012 airfoil templates. Care should be taken to ensure the trailing edges of the root and tip templates are aligned prior to cutting the foam so that the proper leading edge sweep

61

is obtained on the upper part of the vertical fin. Two, short, non-tapered sections will also have to be cut out to provide for that area of the vertical fins below the horizontal tail. All four airfoil sections should be left intact and both sides glassed with two plies of uni-directional and one localized ply of bi-directional fiberglass. The vertical tails will be mounted to the horizontal tail following similar procedures as described in chapter 20 of Reference 24.

VII. ESTIMATED PERFORMANCE AND POWER REQUIRED

To get an estimate of the performance and power required of a vehicle requires some method of estimating the total drag created by the vehicle as it moves through the atmosphere. The total drag is made up of two parts, parasitic and induced drag. Parasitic drag contains not only the profile drag of the wing but also the friction and pressure drag of the tail surfaces, fuselage, engine nacelles, landing gear, and any other component of the airplane which is exposed to the airflow [Ref. 16:p. 251]. The induced drag is created due to the aircraft developing lift. The method used to analyze and estimate the drag is outlined on pages 202-216 of Reference 12.

A. PARASITE DRAG

The parasite drag is estimated by adding together individual drags of different bits of the airplane in contact with the air. The sum is then factored by an amount from 1.4 to 1.7 to account for interference, junctions, and any "bolt-on" accessories that might have been added. The bulk of such drag is caused by struts, wires, landing gear, powerplant and cooling. Also included is leakage drag which is caused by local flow between flap, wing, tail, and control surfaces. [Ref. 12:p. 202]

Equation #18 allows for the determination of the effect the different parts of an aircraft have on total drag by calculating the drag area of any part and adding them all together.The term $C_{D\pi}$ is the individual part drag coefficient obtained from page 210 of Reference 12 and A_π is the area upon which that coefficient is based. The values selected for the individual drag coefficients correspond to the average of the suggest range. By utilizing composites these values should be easily attained.

For the cantilevered wing a value of 0.007 was selected based upon the planform area of 14.375 ft.^{2} The coefficient for the horizontal tail is 1.3 times that value used for the wing or 0.0091 based upon the planform area of 2.76 ft.^{2} $C_{D\pi}$ for the vertical tails is also 0.0091 and an area of 1.467 ft.^{2} was used. A value of 0.100 was estimated for the fuselage based upon the frontal area of 1.047 ft.^{2} The booms have a total area of 0.00417 ft.^{2} each and a coefficient of friction of 0.05 which brings the basic parasite area (f_b) to a value of 0.244. Equation #19 was used to determine the total equivalent parasite area. The values used for the various influence factors were; 1.35 for the landing gear factor, 0.3 for the cooling drag factor, 0.05 for the interference factor, 0.05 for the protuberance factor, and 0.05 for the leakage and trim drag factor. A value of 0.439 ft.^{2} was obtained for the total equivalent parasite area. Dividing this value by the wing area will yield C_{Dp} or the minimum parasite drag. C_{Dp} was calculated to be 0.0306.

B. INDUCED DRAG

Part of the minimum parasite drag (C_{Dp}) varies with lift coefficient, but this gets accounted for in the induced part of total drag calculation. The variable that takes this into account is K', the induced drag factor [Ref 12:p. 202]. A value of 1.4 was estimated for K' of this design based on Table 5-7 of Reference 12. Knowing that the aspect ratio is 9.2, Equation #20 allowed for the calculation of C_D.

C. PERFORMANCE ESTIMATE

The performance of the vehicle was estimated by plotting the values of Table 4. against each other. As a check on the values obtained, a plot of C_L^2 vs C_D was made which yielded a value for the slope of 0.048 (Figure 13). Since the slope is equal to $1/(\pi e AR)$ the equation was solved to determine e, Oswald's efficiency

factor. This value was determined to be 0.7208. Reference 19, page 95 states that a typical value of e for most airplanes is between 0.7 to 0.85.

A plot of L/D vs C_L(Figure 14) shows that the maximum L/D (maximum aerodynamic efficiency) attainable of 13 should occur approximately at C_L = 0.8. The thrust required varies inversely as L/D. Hence, minimum thrust required will be obtained when the airplane is flying at a velocity where L/D is a maximum [Ref 16:p. 256]. By cross referencing this L/D value with Figure 15 and Table 4 it can be seen that this should occur at an angle of attack of 1/2 degrees geometric or a velocity of approximately 65 miles per hour. The cruise condition (75 miles per hour), as determined in the stability section, was found to occur at a geometric angle of attack of -1.52 degrees. This equates to a L/D value of approximately 12.4. Equations #9, #21, and #22 were used to compute horsepower required. Figure 15 shows a plot of the horsepower required for a given true velocity. From this graph one can see that it should require approximately two horsepower to power this vehicle during the cruise condition. This value appears to be in error and it very easily could be, especially since the procedure used is heavily dependent on the drag coefficients estimated for the individual components. It must be remembered that this value is for level, unaccelerated flight at sea level. Just to get an idea of how much horsepower is required for a typical general aviation aircraft at approximately the same velocity, Example 6-3 of Reference 16 was examined. It was found that this aircraft required 50.7 horsepower to fly at 100 ft/sec (68.18 miles per hour). This same aircraft had approximately 184 available horsepower. If a ratio of power available to power required is taken for this flight condition, it is found to be 3.63.

TABLE 4. DRAG CALCULATION DATA

α (geo.)	α (abs.)	CL (mph)	Velocity	CD	L/D	H.P. req.
-7.97	0.00	0.00	-	0.030	0	-
-5.60	2.37	0.20	127.81	0.032	6.15	6.65
-4.40	3.56	0.30	104.36	0.035	8.58	3.88
-3.17	4.80	0.42	88.19	0.039	10.74	2.63
-1.93	6.04	0.54	77.78	0.045	12.08	2.06
-0.69	7.28	0.66	70.36	0.051	12.77	1.76
0.55	8.52	0.78	64.72	0.060	12.99	1.59
1.76	9.73	0.89	60.58	0.069	12.91	1.50
3.00	10.97	1.01	56.87	0.079	12.63	1.44
4.22	12.19	1.12	54.00	0.091	12.26	1.41
5.44	13.41	1.23	51.54	0.104	11.84	1.39
6.64	14.61	1.33	49.56	0.116	11.44	1.38
7.84	15.81	1.43	47.79	0.129	11.03	1.38
9.01	16.98	1.52	46.36	0.142	10.66	1.39
10.17	18.14	1.60	45.18	0.154	10.35	1.40
11.29	19.26	1.66	44.36	0.164	10.11	1.40
12.41	20.38	1.72	43.58	0.174	9.89	1.41
13.47	21.44	1.75	43.21	0.179	9.78	1.41
14.53	22.49	1.78	42.84	0.184	9.67	1.42
15.55	23.52	1.79	42.72	0.186	9.63	1.42
16.53	24.49	1.78	42.84	0.184	9.67	1.42

66
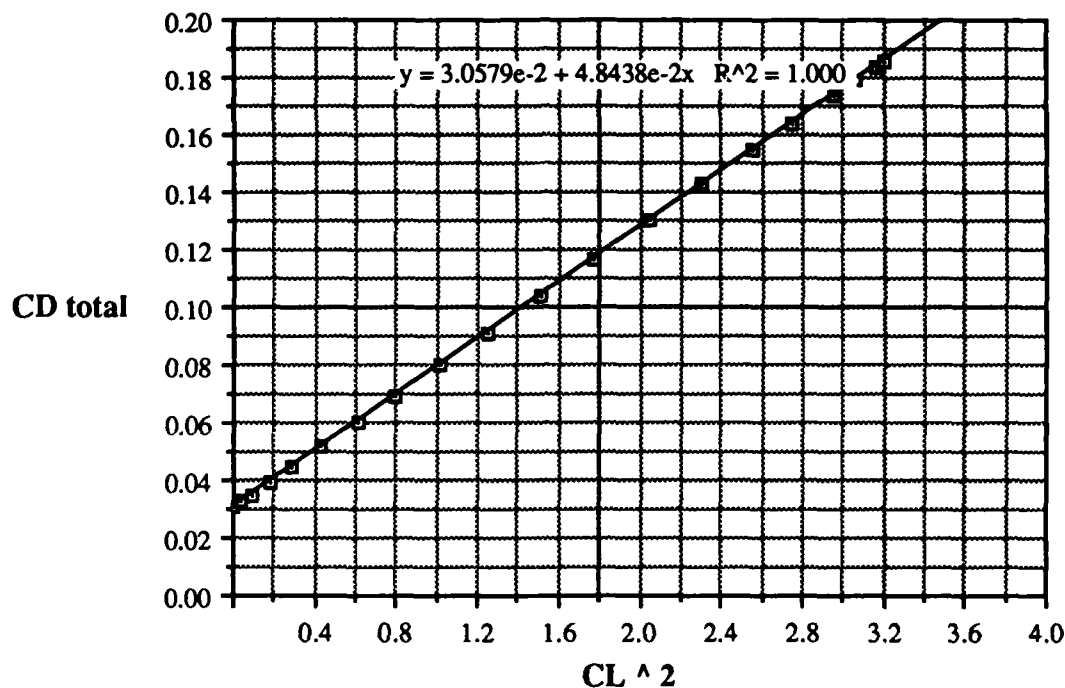
Figure 13. C_{Dtotal} versus C_L^2

If the engine used in this design has approximately 12 horsepower available and assuming a propeller efficiency of 0.65 a power available to power required ratio of 3.9 is obtained. This supports the initial assumption the Limbach L 275E engine operating at half throttle should provide adequate power for climb and cruise conditions of flight. More specific performance calculations will be made once the engine and propeller operating charts are obtained.
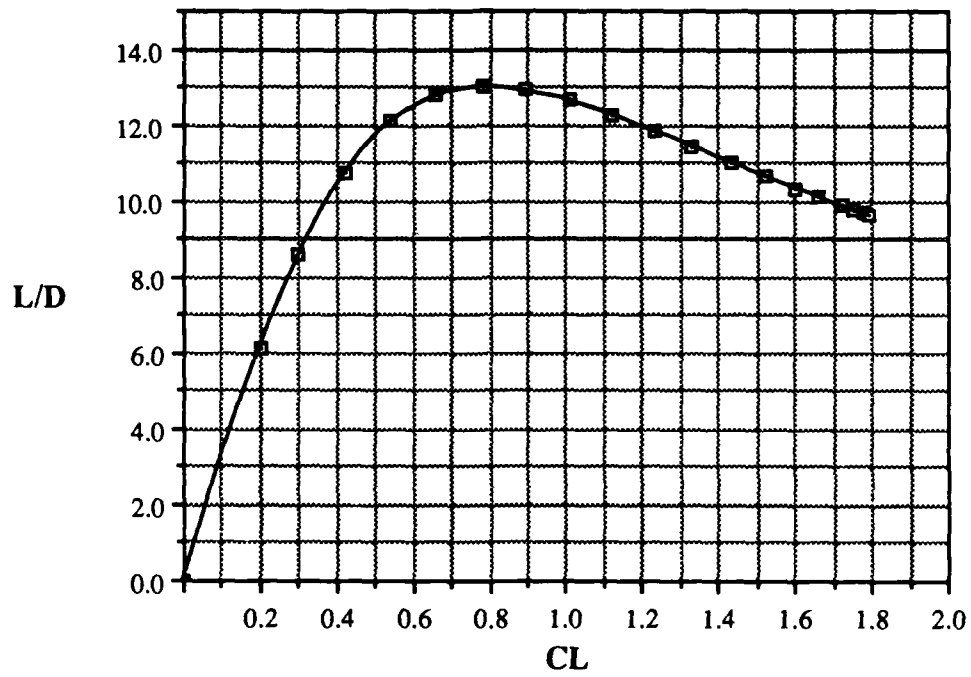
Figure 14. L/D versus C_L
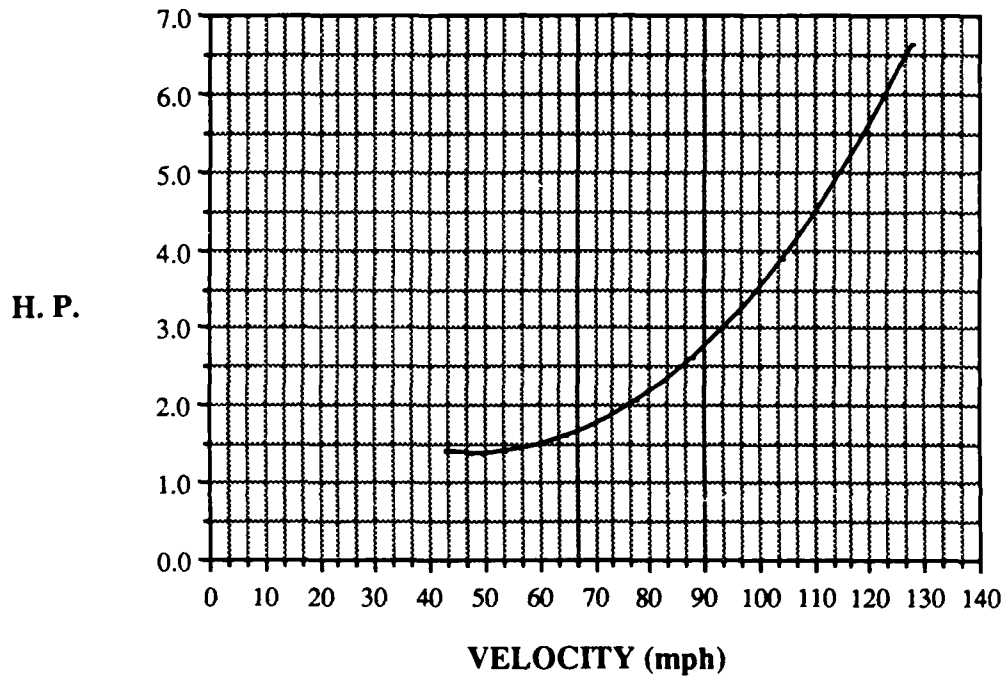
Figure 15. Horsepower Required versus True Velocity

69

VIII.   CONCLUSIONS / RECOMMENDATIONS

A remotely piloted vehicle was designed for the purpose of establishing an RPV flight research program at the Naval Postgraduate School. The airframe design, excluding engine mounting specifics, and minor details, is complete. The wing and empennage structural members were sized by the use of a computer program contained in Reference 15. Stability and initial performance analysis indicate the vehicle should demonstrate positive stability in all axes and possess more than adequate power for all phases of flight.

The amount of work and time required to properly design a vehicle of this type was far greater than initially anticipated and due to this fact, not as much of the construction has been completed as originally thought possible. However, the fuselage was constructed using a technique common to the homebuilt aircraft community and prior to project turn-over major progress is anticipated on the wing construction.

Substantial work, in vastly different areas of interest, such as structural finite element analysis, static load testing, secondary performance analysis, hands-on composite fabrication, design and installation of the flight control system, development of a data acquisition system, and an extensive flight test program remain to be completed.

It is this student's opinion and recommendation that it would prove beneficial to the RPV program, the Department of Aeronautics and Astronautics, and the students involved if this vehicle could be used to conduct joint thesis studies.

The RPV, when completed, will provide an excellent vehicle from which to employ and evaluate low Reynolds number applications and to investigate new

70

aerodynamic phenomena. The RPV will offer students an added element and unlimited possibilities in the conduct of future thesis research. The possession of this vehicle and the establishment of the RPV flight research program will continue to distinguish the Naval Postgraduate School as an outstanding institution of higher learning on the forefront of emerging technology and as one of the few universities in the United States to have such a capability.

APPENDIX A—EQUATIONS

#1

$$(C_M)_{cg} = (C_M)_{ac} + (C_M)_{fuselage} + a_w \alpha_{abs}\left[(h - h_{ac}) - V_H \frac{a_t}{a_w}\left(1 - \frac{\partial \varepsilon}{\partial \alpha} \right)\right] + V_H a_t (i_t + e_0)$$

[Ref. 16:p. 364]

#2

$$R_e = \frac{\rho VL}{\mu}$$

[Ref. 16:p. 134]

#3

$$a_{(2\text{-}d)} = \frac{dC_L}{d\alpha}$$

[Ref. 16:p. 182]

#4

$$a_{(3\text{-}d)} = f\frac{a_e}{1 + \dfrac{(57.3)\, a_e}{\pi\, AR}}$$

[Ref. 18:pp. 11 & 16]

#5

$$\frac{\partial \varepsilon}{\partial \alpha} = 20\left(a_w \lambda^{0.3}/AR^{0.725} \right)(3c/l)^{0.25}$$

[Ref. 12:p. 199]

#6

$$(C_M)_{fuselage} = \frac{k_f W_f^2 L_f}{S_w\, c}\, \alpha_{abs.}$$

[Ref. 19:p. 229]

#7	$(C_M)_{ac} = E\,(Cm)_{ac} - G\epsilon\, a_e\, AR \tan \Lambda$
[Ref. 18:p. 16]	

#8	$V_{trim} = \sqrt{\dfrac{2W}{\rho\, S_w\, C_{L_{trim}}}}$
[Ref. 16:p. 371]	

#9	$e^{\,o}_{tail} = \dfrac{(114.6)C_L}{\pi\,AR}$
[Ref. 19:p. 222]	

#10	$\dfrac{\partial (C_M)_{cg}}{\partial \alpha_{abs.}} = a_w \left[(h - h_{ac}) - V_H\, \dfrac{a_t}{a_w} \left(1 - \dfrac{\partial \epsilon}{\partial a} \right) \right]$
[Ref. 16:p. 366]	

#11	$h_n = h_{ac} + V_H\, \dfrac{a_t}{a_w} \left(1 - \dfrac{\partial \epsilon}{\partial a} \right)$
[Ref. 16:p. 368]	

#12	$\text{Static Margin} = h_n - h$
[Ref. 16:p. 370]	

#13	$(C_{n\beta})_{wing} = -.00006\,(L^o)^{1/2}$
[Ref. 19:p. 318]	

#14	$(C_{n\beta})_{fuselage} = \dfrac{-.96\,K_\beta}{57.3}\left(\dfrac{S_s}{S_w}\right)\left(\dfrac{L_f}{b}\right)\left(\dfrac{h_1}{h_2}\right)^{1/2}\left(\dfrac{w_2}{w_1}\right)^{1/3}$
[Ref. 19:p. 319]	

#15	$$(C_{n\beta})_{w.p.} = \frac{\left[\pi\ D^2\ l_p\ \frac{dCy_p}{d\beta}\ N \right]}{4\ S_w\ b}$$
[Ref. 19:p. 321]	
#16	$$(C_{n\beta})_{v.t.} = (C_{n\beta})_v - \Delta_2\ C_{n\beta}$$
[Ref. 19:p. 324]	
#17	$$(C_{n\beta})_{desirable} = .0005\ (W/b^2)^{1/2}$$
[Ref. 19:p. 326]	
#18	$$f_b = C_{D\pi}\ A_\pi$$
[Ref. 12:p. 204]	
#19	$$f_t = C_{Dp}\ S_w = f_b\ (f_{landing\ gear} + f_{interference} + f_{protuberance} + f_{cooling} + f_{trim})$$
[Ref. 12:p. 207]	
#20	$$C_D = C_{Dp} + (K')\frac{C_L^2}{\pi\ AR}$$
[Ref. 12:p. 202]	
#21	$$Thrust_{req.} = \frac{W}{L/D}$$
[Ref. 16:p. 255]	
#22	$$Power_{req.} = \frac{V\ Thrust_{req.}}{550}$$
[Ref. 16:p. 273]	

WING LOADS

Spar

SPAR SIZING PROGRAM, c. 1984 by M. Hollmann

WING STA,ft.	AIR LOAD,lb/ft.	SHEAR,lb	MOMENT,ft.lbs.
0	34	198	562
.575	34	178	451
1.15	34	158	351
1.725	34	138	278
2.3	34	118	204
2.875	34	99	142
3.45	34	79	
4.025	34	59	
4.6	34	39	
5.175	34	19	
5.75	34	0	0

SPAR SIZING
Enter Tensile or Compressive Strength of Cap, psi?

Spar

Enter Shear Strength of Shear web,psi? 6000

Enter Spar Width, Inches? 3.0

Ener Chord Thickness, % Chord? 17.25

WING STA.ft.	SPAR HEIGHT,in.	CAP THICK,in.	WEB THICK,in.
0	2.07	5.057471E-02	1.594203E-02
.575	2.07	4.096552E-02	1.434763E-02
1.15	2.07	3.236781E-02	1.275362E-02
1.725	2.07	2.478161E-02	1.115942E-02
2.3	2.07	.0182069	9.565217E-03
2.875	2.07	1.264368E-02	7.971015E-03
3.45	2.07	8.09195E-03	5.376811E-03
4.025	2.07	4.551723E-03	4.782608E-03
4.6	2.07	2.02299E-03	3.188406E-03
5.175	2.07	5.057476E-04	1.594204E-03
5.75	2.07	1.08452?E-08	1.228555E-09

Hit Return to Quit?

Tensile Strength - 66,000 PSI

Spar

Enter Shear Strength of Shear Web,psi? 5000

Enter Spar Width, Inches? 3.0
Ener Chord Thickness, % Chord? 17.25

WING STA,ft.	SPAR HEIGHT,in.	CAP THICK,in.	WEB THICK,in.
0	2.07	3.333334E-02	1.594203E-02
.575	2.07	.027	1.434783E-02
1.15	2.07	2.133333E-02	1.275362E-02
1.725	2.07	1.633333E-02	1.115942E-02
2.3	2.07	.012	9.565217E-03
2.875	2.07	8.333334E-03	7.971015E-03
3.45	2.07	5.333331E-03	6.376811E-03
4.025	2.07	2.999999E-03	4.782608E-03
4.6	2.07	1.333334E-03	3.188406E-03
5.175	2.07	3.333336E-04	1.594204E-03
5.75	2.07	7.14802E-09	1.228566E-09

Hit Return to Quit? |

WING PLY CALCULATIONS

Wing Station-ft	Top Cap-in.	Top Cap Plies	Bottom Cap-in.	Bottom Cap Plies	Shear Web-in.	Shear Web Plies
0	0.0505747	5.05747	0.03333334	3.333334	0.01594203	3.188406
0.575	0.0409655	4.096552	0.027	2.7	0.01434783	2.869566
1.15	0.0323678	3.236781	0.02133333	2.133333	0.01275362	2.550724
1.725	0.0247816	2.478161	0.01633333	1.633333	0.01115942	2.231884
2.3	0.0182069	1.82069	0.012	1.2	0.00956522	1.9130434
2.875	0.0126437	1.264368	0.00833333	0.833333	0.00797102	1.594203
3.45	0.0080920	0.809195	0.00533333	0.533333	0.00637681	1.2753622
4.025	0.0045517	0.4551723	0.003000000	0.29999999	0.00478261	0.9565216
4.6	0.0020230	0.202299	0.00133333	0.1333334	0.00318841	0.6376812
5.175	0.0005057	0.05057476	0.00033333	0.033333336	0.00159420	0.3188408
5.75	0.0000000	0.000000108	0.000000001	0.00000007149	0.00000000	0.0000002457

COMPRESSION STRENGTH - 43,500 PSI

Spar

Enter Shear Strength of Shear web,psi? 6000

Enter Spar Width, inches? 3.5
Ener Chord Thickness, % Chord? 22.25

WING STA,ft.	SPAR HEIGHT,in.	CAP THICK,in.	WEB THICK,in.
0	2.67	4.582942E-02	1.685393E-02
.575	2.67	3.712182E-02	1.516854E-02
1.15	2.67	2.930862E-02	1.348315E-02
1.725	2.67	2.245641E-02	1.179775E-02
2.3	2.67	1.649859E-02	1.011236E-02
2.875	2.67	1.145735E-02	8.426967E-03
3.45	2.67	7.332704E-03	6.741574E-03
4.025	2.67	4.124452E-03	5.05618E-03
4.6	2.67	1.833179E-03	3.370787E-03
5.175	2.67	4.582985E-04	1.685394E-03
5.75	2.67	-2.095371E-09	1.904968E-09

Hit Return to Quit?

SPAR BOX BOTTOM CAP

Spar   TENSILE STRENGTH - 66,000 PSI

Enter Shear Strength of Shear Web,psi? 6000

Enter Spar Width, inches? 3.5
Ener Chord Thickness, % Chord? 22.25

WING STA,ft.	SPAR HEIGHT,in.	CAP THICK,in.	WEB THICK,in.
0	2.67	3.020575E-02	1.685393E-02
.575	2.67	2.446665E-02	1.516654E-02
1.15	2.67	1.933168E-02	1.348315E-02
1.725	2.67	1.480082E-02	1.179775E-02
2.3	2.67	1.087407E-02	1.011236E-02
2.875	2.67	7.551438E-03	8.426967E-03
3.45	2.67	4.832918E-03	6.741574E-03
4.025	2.67	2.718524E-03	5.056184E-03
4.6	2.67	1.298232E-03	3.370787E-03
5.175	2.67	3.029604E-04	1.685394E-03
5.75	2.67	4.750045E-09	1.904968E-09

Hit Return to Quit?

SPAR BOX PLY CALCULATIONS

Wing Station-ft	Top Cap-in.	Top Cap Plies	Bottom Cap-in	Bottom Cap Plies	Shear Web-in	Shear Web Plies
0	0.0452294	4.582342	0.03020575	3.020575	0.01685393	3.370786
0.575	0.0371218	3.712183	0.02446666	2.446666	0.01516854	3.033708
1.15	0.0293308	2.933082	0.01933168	1.933168	0.01348315	2.69663
1.725	0.0224564	2.245641	0.01480082	1.480082	0.01179775	2.35955
2.3	0.0164986	1.649859	0.01087407	1.087407	0.01011236	2.022472
2.875	0.0114574	1.145735	0.00755144	0.7551438	0.00842697	1.6853934
3.45	0.0073327	0.7332704	0.00483292	0.4832918	0.00674157	1.3483148
4.025	0.0041247	0.4124655	0.00271852	0.271852	0.00505618	1.011236
4.6	0.0018332	0.1833179	0.00120823	0.1208232	0.00337079	0.6741574
5.175	0.0004583	0.04582985	0.00030206	0.03020604	0.00168539	0.3370788
5.75	0.0000000	0.00000072	0.00000000	0.0000004750	0.00000000	0.00000003810

APPENDIX C—HORIZONTAL TAIL STRUCTURAL CALCULATIONS

HORIZONTAL TAIL LOADS   Spar

SPAR SIZING PROGRAM, c. 1984 by M. Hollmann

WING STA.,ft.	AIR LOADS,lb/ft.	SHEAR,lb	MOMENT,ft.lbs.
0	45	90	35
.1945	45	81	22
.389	45	72	14
.5835	45	63	9
.778	46	54	3
.9725	45	45	2
1.167	46	36	1
1.3615	46	27	1
1.555	45	18	1
1.7505	46	9	0
1.945	46	0	0

SPAR SIZING
Enter Tensile or Compressive Strength of Cap, psi?

Spar

Enter Shear Strength of Shear Web,psi? 5000

Enter Spar Width, inches? 1.5
Ener Chord Thickness, % Chord? 15

WING STA,ft.	SPAR HEIGHT,in.	CAP THICK,in.	WEB THICK,in.
0	1.01952	3.157673E-02	1.471281E-02
.1945	1.01952	2.577715E-02	1.324152E-02
.389	1.01952	2.020911E-02	1.177024E-02
.5835	1.01952	1.547259E-02	1.029896E-02
.778	1.01952	1.137562E-02	8.827684E-03
.9725	1.01952	7.894184E-03	7.356403E-03
1.167	1.01952	5.052278E-03	5.885123E-03
1.3615	1.01952	2.841908E-03	4.413842E-03
1.556	1.01952	1.263066E-03	2.942562E-03
1.7505	1.01952	3.157652E-04	1.471283E-03
1.945	1.01952	0	2.49444E-09

Hit Return to Quit?

Spar

Enter Shear Strength of Shear Web,psi? 6000

Enter Spar Width, inches? 15
Ener Chord Thickness, % Chord? 15

WING STA,ft.	SPAR HEIGHT,in.	CAP THICK,in.	WEB THICK,in.
0	1.01952	2.081193E-02	1.471281E-02
.1945	1.01952	1.685767E-02	1.724152E-02
.389	1.01952	1.331964E-02	1.177024E-02
.5835	1.01952	1.019785E-02	1.029896E-02
.778	1.01952	7.492296E-03	5.827684E-03
.9725	1.01952	5.202984E-03	7.356403E-03
1.167	1.01952	3.32991E-03	5.885123E-03
1.3615	1.01952	1.873076E-03	4.413842E-03
1.556	1.01952	8.324753E-04	2.942562E-03
1.7505	1.01952	2.081179E-04	1.471283E-03
1.945	1.01952	0	2.49444E-09

Hit Return to Quit?

HORIZONTAL TAIL PLY CALCULATIONS

H.T. Station-ft	Top Cap-in.	Top Cap Plies	Bottom Cap-in	Bottom Cap Plies	Shear Web-in	Shear Web Plies
0	0.0315767	3.157673	0.02081193	2.081193	0.01471281	2.942562
0.1945	0.0255772	2.557715	0.01685767	1.685767	0.01324152	2.648304
0.389	0.0202091	2.020911	0.01331964	1.331964	0.01177024	2.354048
0.5835	0.0154726	1.547259	0.01019785	1.019785	0.01029896	2.059792
0.778	0.0113676	1.136762	0.00749230	0.7492296	0.00882768	1.7655368
0.9725	0.0078942	0.7894184	0.00520298	0.5202984	0.00735640	1.4712806
1.167	0.0050523	0.5052278	0.00332991	0.3329991	0.00588512	1.1770246
1.3615	0.0029419	0.2841909	0.00187308	0.1873076	0.00441384	0.8827684
1.556	0.0012631	0.1263066	0.00083249	0.08324753	0.00294256	0.5885124
1.7505	0.0003158	0.03157652	0.00020612	0.02081179	0.00147128	0.2942566
1.945	0	0	0	0	0.00000000	0.00000004989

REFERENCES

1. Sweetman, B., "Unmanned Air Vehicles Make a Comeback," International Defense Review, v. 18, n. 11, November 1985.

2. Gwynne, P., "Remotely Piloted Vehicles Join The Service," High Technology, v. 7, n. 1, January 1987.

3. Parker, CDR D. M., "The Empty Cockpit," Naval Aviation News, v. 70, n. 2, January-February 1988.

4. Aderhold, J. R, Gordon, G., and Scott G. W , Civil Uses of Remotely Piloted Aircraft (Summary Report), NASA CR-137895, July 1976.

5. Evans, JO2 J. L., "RPVs - A Source of Real-Time Intelligence," Naval Aviation News, v. 70, n. 2, January-February 1988.

6. Sweetman, B., "Navy Leads U.S. Unmanned Aircraft Advance," Interavia, v. XLII, n. 10, October 1987.

7. Morrocco, J. D., "Short-Range RPV Passes Navy Review," Aviation Week & Space Technology, v. 127, n. 24, December 14, 1987.

8. Stollery, J. L. and Dyer, D., "The Proof of the Pudding ...Flight Test Data from a Remotely Piloted Vehicle (X-RAE 1)," Aerogram,Vol. 5 No.1, November 1987.

9. McD. Galbraith, R. A., "The Aerodynamic Characteristics of a GU25-5(11)8 Aerofoil for Low Reynolds Numbers," Experiments in Fluids 3, 1985.

10. Bragg, M. B. and Gregorek, G. M., Experimental Study of Airfoil Performance with Vortex Generators, American Institute of Aeronautics and Astronautics, Inc., May 1987.

11. Roskam, J., Airplane Design - Part II, Preliminary Configuration Design and Integration of the Propulsion System, Roskam Aviation &Engineering Corporation, Ottawa, KS, 1985.

12. Stinton, S., The Design of the Aeroplane, Van Nostrand Reinhold Company Inc., New York, NY, 1985.

13. Raymer, D., Aircraft design notes used as textbook for AE 4273 Aircraft Design course, Naval Postgraduate School, Monterey, CA, winter quarter 1988.

14. Thurston, D. B., *Design For Flying*, McGraw-Hill Book Company, 1978.

15. Hollmann, M., *Modern Aircraft Design*, Aircraft Designs, Inc., Cupertino, CA, 1985.

16. Anderson, J. D., *Introduction to Flight*, McGraw-Hill Book Company, 1985.

17. Miley, S. J., *A Catalog of Low Reynolds Number Airfoil Data for Wind Turbine Applications*, Department of Aerospace Engineering, Texas A & M University, College Station, TX, February, 1982.

18. Abbott, I. H. and Von Doenhoff, A. E., *Theory of Wing Sections*, Dover Publications, Inc., New York, NY, 1959.

19. Perkins, C. D. and Hage, R. E., *Airplane Performance Stability and Control*, John Wiley and Sons, Inc., New York, NY, 1949.

20. Althaus, D. and Wortmann, F. X., *Stuttgarter Profilkatalog I*, Friedr. Vieweg and Son, Braunschweig, Wiesbaden, West Germany, 1981.

21. Dommasch, D. O., Sherby, S.S. and Connolly, T.F., *Airplane Aerodynamics, 3rd edition*, Pitman Aeronautical Publications, New York, NY, 1961.

22. Lambie, J. H., *Composite Construction for Homebuilt Aircraft*, Aviation Publishers, Hummelstown, PA, May 1984.

23. Downie, Don and Julia, *The Complete Guide to Rutan Aircraft*, 2nd edition, Tab Books Inc., Blue Ridge Summit, PA, 1984.

24. Rutan, B., *Long - Ez Plans, Section I*, Rutan Aircraft Factory Inc., Mojave, CA, March 1980.

INITIAL DISTRIBUTION LIST

<div align="right">Copies</div>

1. Defense Technical Information Center..2
   Cameron Station
   Alexandria, VA   22304-6145

2. Library, Code 0142..2
   Naval Postgraduate School
   Monterey, CA   93943-5002

3. Chairman 1
   Department of Aeronautics, Code 67
   Naval Postgraduate School
   Monterey, CA   93943-5000

4. Commander..1
   Naval Air Systems Command
   Washington, DC   20360

5. Commander..1
   Pacific Missile Test Center
   Pt. Mugu, CA   93041

6. Commander..1
   Naval Air Systems Command
   UAV Program Office (PMA 263M)
   Washington, DC   20360

7. Naval Research Lab...1
   Code 5712
   4555 Outlook Ave. SW
   Washington, DC   20375

8. Prof. R. M. Howard..5
   Department of Aeronautics, Code 67Ho
   Naval Postgraduate School
   Monterey, CA   93943-5000